Charm Meson lifetime Measurements

A Thesis Submitted
In Partial Fulfillment of the Requirements
for the Degree of ***Master of Science (Research)***

GUIDE: Dr. Minakshi Nayak
CO-GUIDE: Prof. Sudhir Vempati
Center for High Energy Physics

Adithya Ponnuraj

(Roll No.: 11-01-00-10-91-21-1-20420)

to the

Center for High Energy Physics, Physics Department,

Indian Institute of Science, Bengaluru.

April, 2026

Certificate

This is to certify that the Master's project titled "Charm Meson Lifetime Measurement" submitted by Adithya Ponnuraj (Sr No. 11-01-00-10- 91-21-1-20420) to Indian Institute of Science, Bangalore towards partial fulfilment of requirements for the award of degree of Master of Science (Research) in Physics is a record of bona fide work carried out by him under my supervision and guidance during Academic Year, 2025-26.

Dr. Minakshi Nayak
Center for High Energy Physics, Physics Department,
Indian Institute of Science, Benglauru, India

April, 2026

Declaration of Authorship

I, Adithya Ponnuraj, declare that this project titled, "Charm Meson Lifetime Measurement" and the work presented in it are my own. I confirm that:

- This work was done wholly or mainly while in candidature for a research degree at this University.
- Where any part of this thesis has previously been submitted for a degree or any other qualification at this University or any other institution, this has been clearly stated.
- Where I have consulted the published work of others, this is always clearly attributed.
- Where I have quoted from the work of others, the source is always given. With the exception of such quotations, this thesis is entirely my own work.
- I have acknowledged all main sources of help.
- Where the thesis is based on work done by myself jointly with others, I have made clear exactly what was done by others and what I have contributed myself.

Adithya Ponnuraj
Roll No. 11-01-00-10-91-21-1-20420
BS-MS (Research) Programme
CHEP, Physics Department,
Indian Institute of Science,
Bengaluru, 20420, India.

12th April, 2026

Acknowledgements

I take this opportunity to express my immense gratitude to my thesis supervisor, Dr. Minakshi Nayak of the Centre for High Energy Physics at the Department of Physics for her invaluable guidance, unwavering support and near-infinite patience throughout the course of my 2 years as her student. It has been an incredible privelege to pursue this thesis under her mentorship and work in the field of computational high energy physics.

I thank my grandfather, whose birth anniversary was yesterday, for starting me down the path of science and weighting my every blow.

I thank my parents, for showing me that the guardian statues shall always be insurmountable, and to find comfort in it.

I thank Ananya Ramachandran, for reminding me that our ports are of our own choosing, and in it we find the strength to live on.

I thank Anshul Kabra and Tanisha Kumar, for proving to me that even the Night Guard is allowed to sleep.

I thank Aniket Ray for reassuring to me that even escapism can have impermanence and in it, company.

I thank Adithi Amarnath and Romank Chandra Yadav, for showing me what an invincible bulwark is, and I shall forever be inspired by it.

I thank Dithya Vinod, for teaching me that the morning exists because of, and not in spite of, the night.

Lastly, I thank you, the one who reads this, for giving all of this effort meaning.

Adithya Ponnuraj

Contents

List of Figures

List of Tables

Abbreviations

MC	**M**onte **C**arlo
BDT	**B**oosted **D**ecision **T**ree
PDF	**P**robability **D**ensity **F**unction
FOM	**F**igure **O**f **M**erit

For Those Who Come After..

Chapter 1

Introduction

1.1 Introduction

The research into heavy-flavored hadrons has been crucial to the development and verification of the Standard Model of elementary particles. In this respect, studying the charm mesons allows one to explore weak-strong interaction relations on the hadronic level. The accurate determination of the parameters of the mesons, including their lifetimes and decay probabilities, can serve as an excellent test ground for various theories, among which the Heavy Quark Expansion and non-perturbative effects of QCD should be mentioned.

The neutral charm meson, D^0, deserves special attention owing to its phenomenological properties. Being the only neutral meson built from up-quarks, the D^0 system is perfect for investigating weak decays, mixing phenomena, and CP violation in the charm quark sector. Although CP violation in charm is unlikely to exceed 0.1% according to the predictions of the Standard Model, the exact measurements of its value still prove necessary.

The lifetime of the D^0 meson is a basic observable which directly depends on the total decay width of this particle. Lifetime measurements have several important applications: They are used to test the theory, provide input parameters for analyses of mixing and CP violation phenomena, and verify the methods for more complex time-dependent analyses. For obtaining precise values of lifetimes, one needs proper account of detector resolution effects, contributions of backgrounds, and systematic uncertainties connected with decay time measurements.

Electron-positron collider experiments, particularly at the KEKB accelerator with the Belle II detector, at the charm and bottom production threshold conditions offer unique advantages for conducting such measurements. The known composition of the initial state, the presence of negligible backgrounds, and efficient vertexing possibilities make it possible to measure short-lived charm particles accurately. Specifically, measurement of the lifetime of D^0 mesons coming from the cascade decay of $D^{*+} \to D^0\pi^+$ allows one to employ the technique of flavor tagging and minimize combinatorial background contribution. However, the other decay channels of D^0 are also significant in understanding a full picture of D^0 decay.

Although the promising conditions provided by the experiment, there still exist certain difficulties when carrying out precise lifetime measurements. For example, background contributions due to the continuous spectrum production, misreconstructions of charm decays, and purely accidental track associations may bias the decay time distribution unless their contribution is appropriately reduced or considered in the fit. Besides, since the measurement is sensitive to the detector resolution, one has to take into account the resolution effects, and preferably, on an event-by-event level. With the increasing size of collected datasets, the corresponding analysis has to become more complicated.

In this thesis, an accurate measurement of the D^0 meson lifetime has been carried out on a generic MC dataset (to simulate ground readiness) using decays of reconstructed D^0 mesons associated with D^* mesons produced in 5 different hadronic decay channels. Traditional approaches of reconstructing and analyzing decays are combined with advanced multivariate tools for suppression of background contributions. To improve the purity of selected sample, the machine learning-based classifier is applied. Invariant mass fits were used for the estimation of signal fractions in various kinematic bins where lifetimes have been measured. Decay time distribution was reconstructed with unbinned likelihood approach which included uncertainties in decay times per event and the resolution function. The decay of the K_S meson, which is one of the daughter particles in 2 of the 5 decay channels in this analysis is also studied in this thesis, in order to understand FastBDT suppression efficiencies of neutral candidate particles on the basis of geometric and kinematic event variables.

1.2 Problem Statement

Measurement of the D^0 lifetime precisely depends on correct identification of the decay vertex, on accurate determination of the decay time uncertainty, and on rejection of the background contribution. While electron–positron collider environment offers fairly clean conditions for experimental measurements, background contamination due to continuum processes as well as mis-reconstruction of the charm decays can be still sizable and cause deviation in the time distribution if not carefully treated. The main issue that is investigated in this thesis is how to extract a correct D^0 lifetime measure taking into account the possible experimental effect mentioned above.

The main difficulty in measuring the D^0 lifetime is the multi-channel nature of this particle. Namely, the D^0 meson is reconstructed via several decay modes with different kinematics, detector response, and background level. While there exists an analysis strategy that works successfully in some decay topologies, the same method can fail to work efficiently in another decay mode. This problem needs to be solved by developing a consistent analysis technique.

The background suppression is a critical part of this problem. Simple cuts on the features cannot effectively use the information contained in the multi-dimensional feature space. In order to maximize this, advanced multivariate analysis techniques should be used in order to make the most effective use of the signal event variable distributions, and minimize the loss of the purity of the signal. In addition, the type of classifier that is chosen may introduce an additional source of bias to the experiment, and therefore, should be studied first.

Another basic element of the problem is modeling of the decay time resolution. Detector resolution and fluctuating accuracy of each event vertex reconstruction make the decay time distribution smeared. Neglecting this effect leads to a systematic shift in the lifetime measured. Thus, the solution to the problem includes the fitting technique capable of handling uncertainty in each individual decay time in each channel independently of other channels.

Last but not least, lifetime extraction crucially depends upon the ability to accurately discriminate between signal and background components. Independent signal fractions should be calculated and correctly applied in the subsequent analysis of decay times. This requires an appropriate handling of mass spectra, background modeling, and interrelations with the decay-time likelihood function.

In conclusion, the main focus of this thesis is to develop an analysis approach, incorporating multivariate background rejection, signal purity assessment, and resolution effects during the decay time fit, aiming at the determination of the lifetime of the D^0 meson through different decay channels.

1.3 Thesis Organization

The thesis is structured as follows. Chapter 1 starts with discussing the physics motivations for the research, presenting the problem that is considered and providing an outline for the thesis. Chapter 2 provides an introduction to the theoretical and experimental aspects of the research, with focus on the properties of charm mesons and lifetimes.

Chapter 3 discusses experimental setup used in the research and the data samples analyzed in the thesis, focusing on the detector sub-systems important for the reconstruction of decay vertices and describing data processing scheme. Chapter 4 discusses event reconstruction procedure and analysis methods in general, presenting decay channels selected for the analysis and decay-time observables used.

Chapter 5 focuses on background suppression using multivariate analysis techniques. The implementation of the primary classifier is discussed, along with comparisons to alternative machine-learning approaches and the optimization of selection criteria. It also covers the K_S MVA background suppression and it's potential use in the main analysis. Chapter 6 presents the signal extraction and lifetime fitting procedure, including invariant mass modeling, resolution effects, and the extraction of the D^0 meson lifetime.

Finally, Chapter 7 summarizes the results of the analysis, discusses their implications, and outlines possible directions for future improvements and extensions of this work.

Chapter 2

Literature Review and Physics Background

2.1 Introduction

Lifetime determinations in charm mesons have provided a key experimental arena for testing both methods and the theory of heavy flavor physics for decades now. Lifetime observables, being fundamental in nature, explore the total widths of hadrons and thus serve as crucial input in the investigation of phenomena related to flavor mixing and CP violation in addition to providing insights into nonperturbative aspects of QCD. Charm lifetime observables have been especially informative due to the fact that the charm quark mass is in the range where neither the perturbative treatment nor the use of phenomenology can yield accurate predictions on its own. This makes high-precision experimental observations invaluable for assessing the quality of various theoretical frameworks such as HQE.

It should be noted that the development of lifetime measurements in charm mesons has been closely correlated with the evolution of experimental techniques. The ability of fixed target experiments to reconstruct displaced charm decays was confirmed in early investigations. With collider-based experiments, one could obtain more favorable background conditions and better vertex resolution and reconstruction efficiency.

One of the conceptual breakthroughs in charm physics experiments is that of moving from cut-based analysis methods to more sophisticated likelihood and multivariate analysis techniques. As detectors evolved and collected larger amounts of data, older methods were found to be inadequate for extracting all the relevant information. This breakthrough included using unbinned maximum likelihood techniques to extract meson decay times, while taking uncertainties on a case-by-case basis and employing more realistic resolution functions. Lifetime studies have therefore benefitted from a large reduction in systematics.

The other development in recent years has been that of new high-luminosity colliding-beam machines and their use in charm physics experiments, like the upgradation of the Belle Project to the Belle II Project. Asymmetrical electron-positron colliders have made possible studies involving charmed mesons produced at high boosts as well as excellent separation of vertexes. Hadron collider machines, on the other hand, provided large samples of charmed particles due to their high production cross-sections.

The advent of machine learning in high-energy physics research has brought about a revolution in the experimental methodology. Modern charm meson studies commonly involve the application of multivariate classifiers such as boosted decision trees. This technique is especially useful when it comes to signal identification and background suppression if background processes are complex enough and exhibit some level of correlation between several observables. The increasing popularity of machine learning is a reflection of changing approaches to high-dimensional data analyses aiming to maximize selection efficiency and statistical precision.

Against this backdrop, modern experiments attempt to enhance the precision of measurements in charm particle lifetime determinations with a combination of cutting-edge detector technology and data analysis methodology. Resolution-corrected fits, control of the potential contamination with background events, and validation techniques that allow avoiding the influence of a theoretical model on the outcome of the experiment are among those employed in contemporary charm meson lifetime calculations.

The evolution of experiments measuring the lifetimes of charm mesons through time will be outlined in this chapter, emphasizing important advances that have been achieved in the area and the main experimental breakthroughs. Emphasis will be given to the transition from early fixed target experiments to collider-based methods and the use of more complex analysis techniques, such as multivariate methods. The content of this chapter is essential background for the analysis carried out in subsequent chapters.

2.2 Literature Review

First experimental measurements of charm meson lifetimes have been performed in fixed target experiments, where high energy hadron beams interacted with stationary nuclear targets. In particular, the pioneer work in this area was performed in the experiment E687 at Fermilab, which showed that silicon microstrip detectors can be used to make displaced decay vertex reconstruction of charm hadrons with sufficient spatial resolution for lifetime measurement [E687]. The challenging aspects of this experiment include high track multiplicities and a substantial amount of hadronic background. Nonetheless, the experiment managed to achieve competitive precision in lifetime measurement due to vertex separation and proper background treatment.

Switching to electron–positron collider experiments brought a notable improvement of experimental conditions. The experiment CLEO made use of its advantage of having an environment with fewer particles than in fixed target experiments along with known kinematical properties of produced particles [CLEO]. The disadvantage of small boost, which makes possible poor vertex separation in comparison with later experiments, was overcome by excellent tracking capabilities. CLEO measurements helped improve previous lifetime measurements and reached greater agreement between the decays of different types. It also became evident in the experiment that detector resolution effects should be taken into account.

An important breakthrough in the precision of charm lifetime measurements was achieved due to the emergence of asymmetric B-factories, such as BaBar and Belle. Using asymmetric beams of electrons and positrons allowed one to obtain boosted charm mesons, which provided significant improvements in the spatial resolution of production and decay points [BaBar, Belle]. Thanks to high luminosity and modern vertex detectors, these measurements could be performed with unprecedented accuracy. In both experiments, an unbinned maximum likelihood analysis of the distribution of proper decay times along with resolution models of the detector was used. Due to a sufficiently large number of events in the sample, possible systematic effects could be investigated very thoroughly.

In the epoch of hadron colliders, a different method for charm physics emerged. Designed specifically for heavy flavors, the LHCb experiment utilized a huge charm production cross-section in proton-proton collisions and the design of the vertex detector, the Vertex Locator (VELO), optimal for vertex reconstruction [LHCb].

Despite challenging conditions in a hadron collider environment, LHCb performed world's best measurements of the lifetimes of charm mesons and parameters of charm mixing, raising theoretical interest in applying the Heavy Quark Expansion to charm particles. These results demonstrated that, with sufficient detector performance and analysis sophistication, hadron colliders could rival or surpass e^+e^- experiments in lifetime precision.

Moreover, more recently, the Belle II experiment has taken this development further by bringing together the clean experimental conditions of an e^+e^- collider and cutting-edge detector technology [BelleII-Lifetime]. At the SuperKEKB collider, the Belle II experiment uses an advanced vertex detector, which includes a Pixel Detector (PXD) and a Silicon Vertex Detector (SVD). The high-resolution detector allows accurate determination of track impact parameters near the collision point. Initial measurements of the charm meson lifetime at Belle II have shown competitive accuracy even with a limited amount of collected luminosity, thereby validating the detector concept and the measurement technique. In this case, a resolution-dependent fit is used in conjunction with empirical background estimation.

In addition to the evolution of the experimental apparatus, the analysis methodology has undergone significant changes. The use of cut-based methods in analyses provides good reliability but may not make full use of the correlation between the variables, which is especially problematic in studies requiring complex background estimates. As a consequence, multivariate methods have found widespread application in charm physics. For instance, boosted decision trees and other classifiers were used to increase signal purity and reduce the background from continuum processes [FastBDT-Photon].

In addition to the aforementioned applications, machine learning methods have also found success in the selection of neutral strange hadrons, including the Ks meson

[Ks-study]. Traditionally, Ks selection is carried out based on certain requirements to ensure efficient selection at displaced vertex topology and track quality. Although such a method is rather robust, its drawbacks include poor efficiency or purity over broad kinematic ranges.

In order to compensate for some deficiencies inherent to traditional selection procedures, a novel approach based on a neural network was suggested recently, with the algorithm referred to as nisKsFinder [nisKsFinder]. Using the method, an ntuple consisting of different kinematical, topological and vertex qualities characteristics of the decay products is constructed and used by the multivariate classifier for background rejection purposes. As shown in the paper, the suggested selection criterion allows achieving much better results than the goodKs criteria.

Overall, the development of methods for measuring the lifetime of charmed mesons shows consistent progress toward achieving better precision due to improvements in detector technology, statistical precision, and analytical methods. Each stage of research, starting from fixed target experiments and up to collider-based studies, contributed to advancing both experimental procedures and analysis techniques. This study is an example of how these advances can be utilized in order to obtain ever more accurate results regarding the lifetimes of charmed particles.

2.3 Research Gaps

Although there is a large number of publications on charm meson lifetime measurement, several significant shortcomings have been identified in the literature on the subject. The problems in question are related neither to the absence of data nor experimental capabilities, but to the employment of up-to-date techniques, uniformity in decay modes' description, and correction for experimental effects, which may

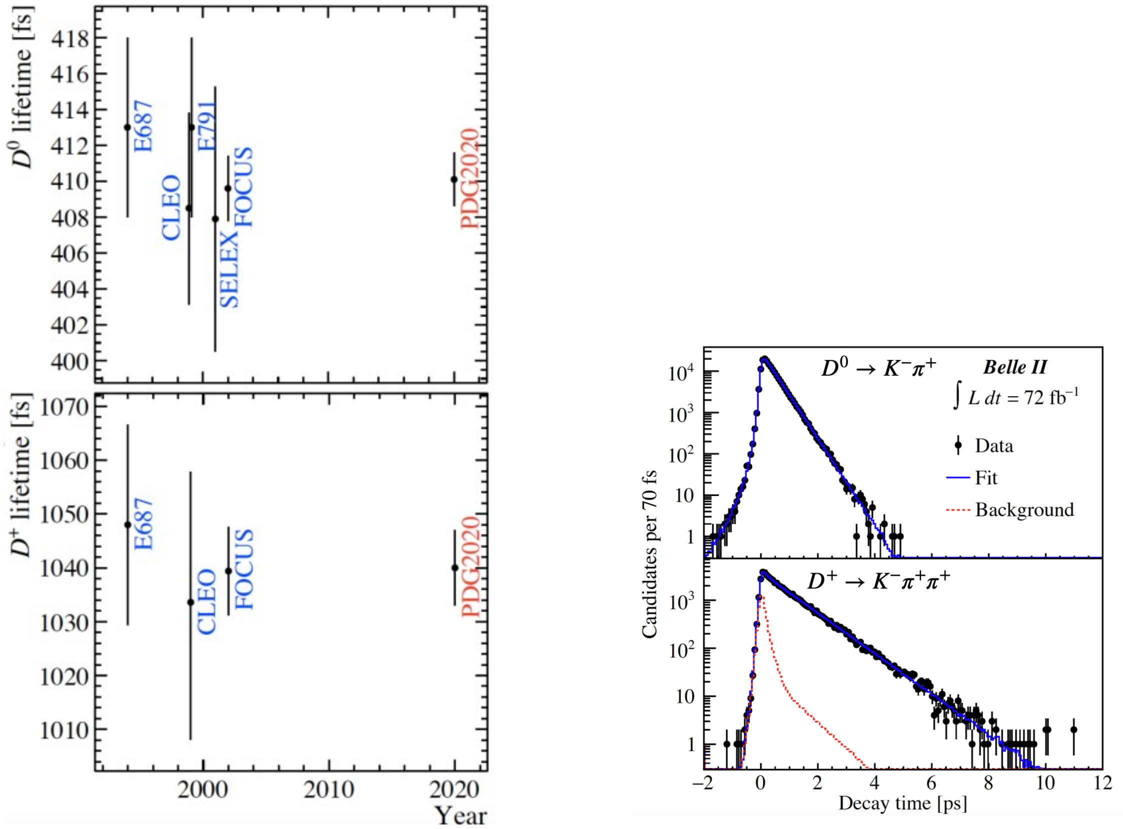

Figure: Plot 1 shows the lifetimes and the year of estimation. Plot 2 shows the fit to the decay time.

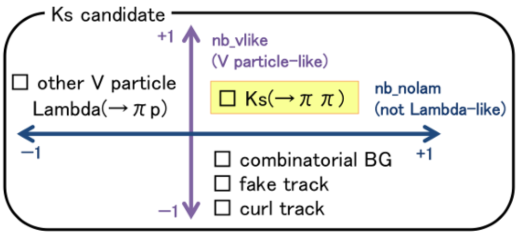

FIGURE 2.1: Kinds of Ks candidate and NeuroBayes outputs

introduce biases into precision measurements. Overcoming those problems is crucial for extracting maximum potential from both current and prospective charm data sets.

First of all, there is a lack of systematics and unification of multivariate analysis application in charm lifetime measurements. Even though the machine learning methods proved their effectiveness in many cases, including charm quark physics—in particular, in suppression of various backgrounds and reconstruction of decay vertices—only partial and auxiliary employment of such algorithms has been observed so far. In several papers, classification models for charm decays were created with respect to each particular channel or source of background independently. As a result, channel-dependent selections bias has become a serious problem.

Despite the presence of a lot of publications on the charm meson lifetime determination, there are a number of important drawbacks that were revealed by the authors in the relevant literature. They have nothing to do with the data unavailability or limitations of experimenters but are associated rather with the application of modern methodologies, consistency of decay channel descriptions, and correction of any experimental biases that might influence precision measurements. Solving those issues is essential in achieving the maximum benefit from current and future measurements.

Above all, there are certain gaps in the systematic approach to the use of multivariate analysis in lifetime determination studies. Despite the success of machine learning approaches shown in many areas, including charm quark physics, where machine learning was used effectively for suppressing different backgrounds and reconstructing the decay vertex position, only partial and supplementary application of such models has been observed so far. In some papers, separate classification models were developed with regard to each channel or each type of background sources.

Moreover, previous investigations have mostly focused on high-statistics single decay modes rather than considering multiple decay channels simultaneously. Modes with small branching ratios and complicated decay products, such as decays leading to displaced neutral hadrons, tend to be omitted or studied independently. Such an approach hampers the possibility of cross-checking the coherence of results obtained from various decay topologies and examining the stability of the analysis procedure in different backgrounds and resolutions.

In addition, there is a larger issue regarding the methodology and scalability of analysis procedures used in modern experimental research. Given the growing size of the datasets produced by current experiments, the algorithms utilized need to be efficient enough, minimize the necessity of using simulations, and be adaptable to changes in detector performance. Some of the previously employed methods may no longer be optimal due to the rapid growth in dataset sizes.

The aim of this thesis is to develop a unified strategy for analyzing and measuring D meson lifetimes using multivariate background suppression, signal coherence estimation, and simultaneous resolution-dependent decay time fitting of multiple decay channels.

Chapter 3

Experimental Setup and Dataset

3.1 Experimental Setup - The Belle II Experiment

The Belle II experiment is a next-generation particle physics detector located at the interaction point of the SuperKEKB electron–positron collider in Tsukuba, Japan. It is designed to study the properties of heavy-flavor hadrons—particularly those containing bottom and charm quarks—with unprecedented precision. Operating in a clean e^+e collision environment, Belle II enables detailed investigations of rare decays, CP violation, lepton flavor universality, and mixing phenomena in the heavy-flavor sector.

Belle II is the successor to the highly successful Belle experiment, which, together with the BaBar experiment at SLAC, played a pivotal role in establishing the Standard Model description of flavor physics. Measurements from Belle provided critical confirmation of the Cabibbo–Kobayashi–Maskawa (CKM) mechanism and precise determinations of CP-violating parameters in the B-meson system. Despite these achievements, the Belle experiment was limited by both dataset size and detector performance, restricting its sensitivity to extremely rare processes and subtle deviations from Standard Model predictions.

To overcome these limitations, Belle II was conceived as a comprehensive upgrade of both the detector and the accelerator. The SuperKEKB collider employs an innovative "nano-beam" scheme that tightly focuses the beams at the interaction point, dramatically increasing the collision rate. With a target instantaneous luminosity of $8 \times 10^{35} cm^{-2}s^{-1}$.

SuperKEKB is expected to deliver data samples more than fifty times larger than those accumulated by Belle over its full operational lifetime. This substantial increase in statistics is essential for advancing precision measurements in heavy-flavor physics.

In parallel with the accelerator upgrade, the Belle II detector was rebuilt with significantly improved subdetectors optimized for modern experimental demands. Enhancements in vertex resolution, tracking efficiency, particle identification, and calorimetry enable more accurate reconstruction of decay vertices, improved particle discrimination, and more effective background suppression. These capabilities are particularly important for charm physics, where precise vertexing and decay-time resolution are critical for lifetime measurements and mixing studies.

An additional advantage of Belle II arises from the clean experimental environment provided by $\mathrm{e^+e^-}$ collisions. In contrast to hadron colliders, where charm hadrons are produced within dense QCD jet backgrounds, Belle II benefits from low event multiplicity and strong kinematic constraints. At center-of-mass energies near the $\Upsilon(4S)$ resonance, processes such as $\mathrm{e^+e^-} \rightarrow c\bar{c}$ produce abundant charm mesons with minimal underlying event activity. This allows for high-purity reconstruction

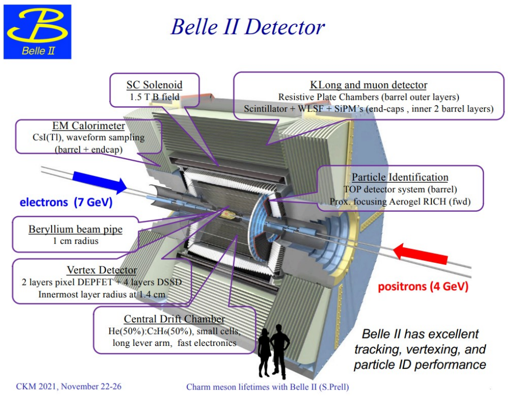

FIGURE 3.1: Belle 2 detector

of charm decays and precise measurements of decay time, invariant mass, and vertex displacement.

The combination of high luminosity, improved detector performance, and a clean collision environment makes Belle II uniquely suited for precision charm physics. In this analysis, these features are exploited to measure the lifetime of the D^0 meson across several hadronic decay modes. The following subsections describe the accelerator, detector subsystems, and experimental infrastructure relevant to this study.

3.1.1 SuperKEKB and the Interaction Point

The Belle II experiment uses the SuperKEKB electron-positron collider, which has been constructed in order to increase the luminosity by approximately forty times compared to its predecessor KEKB. This is mainly accomplished by using the nano-beam concept, which means decreasing the beta value of the beam in the vertical direction by approximately a factor of twenty.

In order to achieve this, it was decided to change the beam crossing angle from 22 to 83 mrad, so that the distance between the interaction point and the last focusing quadrupoles could become smaller. This solves the hourglass problem and allows to avoid the use of combined-function magnets, which are very sensitive to background radiation. Also, additional luminosity increases can be achieved by raising the current and decreasing the beam emittance.

The beam energies were also adjusted, with the positron energy increased from 3.5 GeV to 4.0 GeV and the electron energy reduced from 8.0 GeV to 7.0 GeV. These changes improve beam lifetime by suppressing the Touschek effect and reducing emittance growth from intra-beam scattering. However, they result in a lower Lorentz boost (γ), decreasing from 0.42 to 0.28. This reduction must be carefully accounted for in time-dependent measurements, including lifetime analyses.

The beam pipe radius was reduced from 15 mm in KEKB to 10 mm in SuperKEKB, allowing the vertex detector to be placed closer to the interaction point and significantly improving impact parameter and vertex resolution. Overall, the expected vertex resolution improvement relative to Belle is approximately a factor of two.

Since Belle II uses beams with greater luminosities and currents, it runs under a more difficult background situation. For this reason, a Level-1 trigger system which can process signals at frequencies as high as 30 kHz is used. As for the design of the beam pipe, it consists of a double walled pipe made of beryllium around the interaction point with low radiation lengths. In addition, there is tantalum shielding placed at the crotches in order to diminish electromagnetic shower background events. Finally, the inner surface of the pipe is lined with gold.

3.1.2 Vertex Detector: PXD and SVD

The most inner detector element of the Belle II experiment is the vertex detector made of two layers of the Pixel Detector (PXD) with a surrounding silicon vertex detector comprising four layers. Both detectors provide accurate vertexing capabilities crucial for precision time measurements of particle decays.

The Pixel Detector uses the DEPFET sensor technology, where carriers produced in the silicon structure by passing charged particles are collected in a deep internal potential well and amplify the output transistor current. Such amplification allows the detector elements to be very thin (only 75 μm thick), resulting in fewer multiple scatterings and improved spatial resolution, especially for tracks of low momentum.

For the PXD, custom ASICs are used to handle read-out and digitization. The read-out strategy uses the gating of regions of interest, which greatly reduces the output bandwidth by about an order of magnitude compared to conventional pixel sensors. In addition, the pixel sensors allow the detector to be used in a gated configuration, where charge collection is stopped temporarily during beam injection periods to reduce pile-up effects.

The four-layered system of double-sided silicon strip detectors forming the SVD surrounds the PXD at radial positions of 39 mm, 80 mm, 104 mm, and 135 mm. The additional detector geometry aids in improving tracking performance, allowing for displaced vertex reconstruction such as that from K_S decay. The SVD front-end electronics utilize the APV25 chip, known for its low noise and fast shaping capabilities, along with being radiation hard.

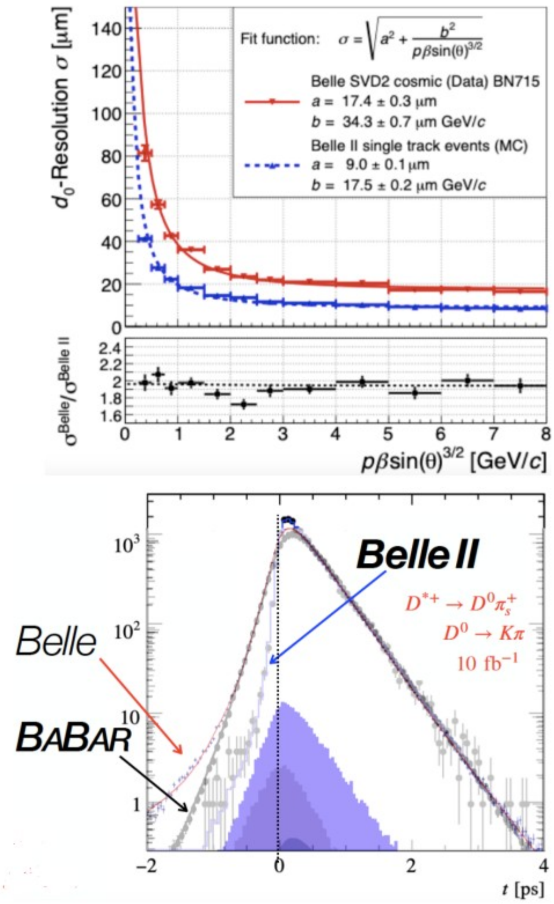

Figure 3.2: SVD: (above) Energy deposition with traversed distance, (below): Resolution function over the years

3.1.3 Central Dift Chamber (CDC)

The CDC is the main tracking device used in Belle II, performing tasks related to the accurate determination of particle momenta, particle identification through energy loss (dE/dx), and trigger information at low momentum. The dimensions of the CDC are cylindrical in shape with an inner radius of 16 cm, an outer radius of 113 cm, and a length of 232.5 cm, using light material design to reduce the impact of multiple scattering.

The 56-layer structure of CDC forms nine superlayers in an alternate axial-stereo geometry, with 14,336 drift cells filled with He-Ethane gas mixture. These drift cells have been designed in such a manner as to achieve fast drift and excellent spatial resolution. Readout is done through front-end electronics developed specifically for this purpose, providing timing and pulse height information simultaneously.

3.1.4 Particle Identification Systems (PID)

Charged particle identification in the Belle II experiment is carried out by two Cherenkov counters—the Time of Propagation (TOP) detector located in the barrel part of the apparatus and the Aerogel Ring Imaging Cherenkov (ARICH) counter placed in the forward end-cap section.

The Time of Propagation (TOP) detector records the arrival times and spatial coordinates of Cherenkov photons generated in quartz radiator blocks. High-quality timing provided by fast micro-channel plate photomultipliers is about 100 picoseconds; thus, separation of particles is performed successfully within a broad momentum range.

In the forward part of the detector, Cherenkov photons from charged particles are detected via aerogel radiator blocks with double refractive indices. Hybrid avalanche photodiodes allow for effective separation of particles, which is necessary in hadron decay modes.

3.2 Dataset and Reconstruction

The analysis presented in this thesis is based on simulated and reconstructed datasets produced within the Belle II software framework. These datasets correspond to electron–positron collision events collected at center-of-mass energies near the $\Upsilon(4S)$ resonance, where charm–anticharm pairs are abundantly produced through the process

$e^+e^- \to c\bar{c}$

The primary focus of this study is on the reconstruction and lifetime measurement of the neutral charm meson D^0, using hadronic decay modes that offer favorable branching fractions and well-defined decay topologies. The dataset contains a mixture of signal events corresponding to correctly reconstructed charm decays and background events arising from random track combinations, continuum processes, and secondary charm production.

Generic Monte Carlo (MC) simulated samples are used extensively throughout this analysis to validate reconstruction performance, estimate efficiencies, and model detector resolution effects. These samples incorporate a detailed detector simulation based on GEANT4, ensuring realistic modeling of particle interactions with detector material, electronic response, and reconstruction effects. Simulated events are processed using the same reconstruction algorithms as applied to experimental data, enabling direct comparison between data and MC distributions.

The dataset is organized into multiple reconstruction channels, each corresponding to a specific decay topology of the D^0 meson. These channels are treated independently in the analysis to account for channel-dependent resolution effects, background composition, and reconstruction efficiencies. The use of multiple channels allows for cross-validation of results and provides a consistency check on the extracted lifetime measurements.

3.2.1 Nature of Dataset and target decay channels

The dataset used in this analysis corresponds to a 200 fb^{-1} generic Monte Carlo (MC) sample generated in systematic production campaigns by the Belle II collaboration. These samples simulate electron–positron collisions at center-of-mass energies near the Υ (4S) resonance and include a realistic mixture of continuum $e^+e^- \to q\bar{q}$ (q=u,d,s,c) processes, as well as detector backgrounds and reconstruction effects.

The MC events are processed through the full Belle II detector simulation and reconstruction chain, ensuring that they accurately reflect detector acceptance, resolution, and efficiency effects. This dataset provides sufficient statistical power to study reconstruction performance, background suppression, and lifetime fitting across multiple decay channels of the D^0 meson.

The analysis focuses on five hadronic decay channels of the D^0 meson, selected based on their branching fractions, reconstruction feasibility, and sensitivity to decay-time measurements:

1. **Channel 1:** $D^0 \to K^+K^-$

   `decayString='D0:ch1 -> K+:good K-:good'`

   A mass cut of $1.75 < M < 2.1$ GeV/c^2 and an $x_p > 0.40$ cut are applied. The "good" tag ensures that only high-quality tracks are considered.

2. **Channel 2:** $D^0 \to \pi^+\pi^-$

   `decayString='D0:ch2 -> pi+:good pi-:good'`

   Identical mass and x_p cuts to Channel 1 are used. The "good" tag filters optimal pion tracks.

3. **Channel 3:** $D^0 \to K^-\pi^+$

   `decayString='D0:ch3 -> K-:good pi+:good'`

   This channel uses the same cuts as Channels 1 and 2, with a focus on selecting well-measured kaon and pion tracks.

4. **Channel 4:** $D^0 \to K_S^0\pi^+\pi^-$

   `decayString='D0:ch4 -> K_S0:good pi+:good pi-:good'`, `cut='1.75 < M < 2.15 and xp > 0.4'`

   The mass window is extended to accommodate the broader kinematics of the K_S^0, while maintaining the same x_p threshold.

5. **Channel 5:** $D^0 \to K_S^0 K^+\pi^-$

   `decayString='D0:ch5 -> K_S0:good K+:good pi-:good'`, `cut='1.75 < M < 2.15 and xp > 0.4'`

   As in Channel 4, this channel includes a K_S^0 in the final state, along with a kaon and pion.

In addition to these D^0 decay modes, a dedicated sample of $K_S^0 \to \pi^+\pi^-$ decays is also reconstructed for standalone studies related to multivariate K_S reconstruction and selection optimization.

3.2.2 Event Preselection and D^0 Vertex Reconstruction

Prior to analyzing the decays by means of a full physics study, it is crucial to employ filtering techniques which discard unphysical and noisy events along with poorly reconstructed events. The main objective at this step is to have a good dataset to be used during the stages of suppressing the continuum component and measuring the lifetime.

The process starts from applying standard event-level quality cuts at the MC datasets during reconstruction. These cuts include conditions related to global event characteristics, such as having a good reconstruction of the primary vertex, the minimal number of charged tracks in the event, and the correctness of the information obtained from different subsystems of the detector. The implementation of these cuts within the basf2 framework is done via several modules including `EventInfoFilter`and GoodTracksSkimFilter.

After the global preselection, the D0 candidates are reconstructed by making use of the channel-dependent decay modes that have been specified through the `ma.reconstructDecay` module. Decay modes that are used include those outlined in Section 3.2.1. Selection cuts based on the invariant mass and scaled momentum x_p, which is the ratio of the momentum of the particle in the center-of-mass system to the maximum possible momentum, are imposed on the decays.

The charged tracks that enter into the reconstruction process are further constrained to satisfy certain particle identification (PID) criteria using the `pidalgo` module. The `pidalgo` function makes use of the likelihoods for various particle hypotheses calculated using information from the TOF, ARICH and CDC dE/dx detectors.

The D^0 vertex reconstruction is done by the VertexFitter module in basf2, which utilizes the Kalman Filter technique to reconstruct the charged daughters' tracks at a common point. The goodness of fit of the vertex is determined by calculating the vertex χ^2 probability, and if the value is below a certain cut-off, then the event is discarded. In cases when there are more than one D^0 reconstructed per event, selection of the best candidate is done by choosing an event with the closest mass to the nominal value of D^0 mass.

3.2.3 Decay Time Reconstruction and Feature Construction

With the best D^0 candidate selected, a comprehensive set of kinematic and geometric observables is computed for each event. The reconstructed decay vertex and the known interaction point are used to determine the D^0 flight vector, which is projected along the reconstructed momentum direction to calculate the proper decay time:

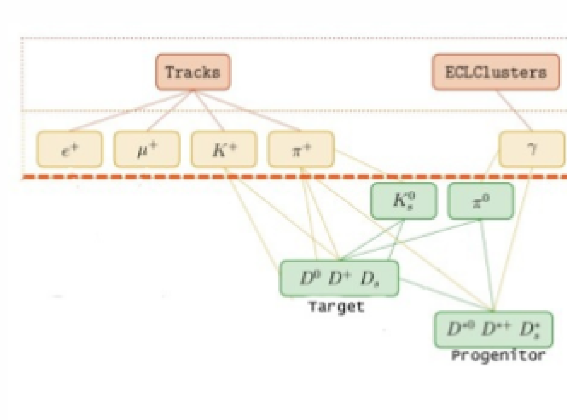

FIGURE 3.3: Reconstruction Pipeline

$$t = \frac{L \cdot M}{\mathbf{p}}$$

where L is the decay length vector, M is the nominal D^0 mass and $|\mathbf{p}|$ is the magnitude of the reconstructed momentum.

The uncertainty on the decay time is estimated on an event-by-event basis using the `FlightLength` and DecayTimeError modules, which propagate uncertainties from the track parameters and vertex fit. This per-event decay time uncertainty plays a crucial role in the lifetime fitting procedure described in later chapters.

In total, 172 kinematic, geometric, and vertex-quality variables are computed for each reconstructed candidate. These include observables such as decay length, decay time, vertex displacement, momentum alignment, PID likelihoods, impact parameters (d_0,z_0), and vertex fit quality indicators. While some of these variables are used directly in preselection cuts, a large subset serves as input features for the multivariate classifiers employed for continuum suppression, discussed in the following section.

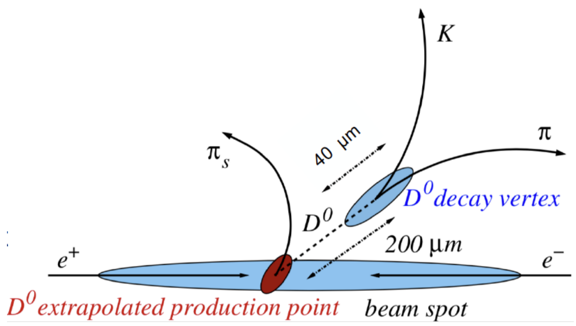

FIGURE 3.4: Reconstructed event track

3.2.4 Preparation of the Analysis Samples

To ensure high purity and consistency in the signal sample used for lifetime measurements, additional selection criteria are applied after reconstruction. Candidates are required to lie within broad invariant mass windows around the nominal D^0 mass—typically $1.75 < M < 2.1$ GeV$/c^2$ for fully charged channels and up to 2.15 GeV$/c^2$ for channels involving K_S mesons. A lower bound on the scaled momentum ($x_p > 0.4$ is imposed to suppress combinatorial background and reduce contamination from secondary charm production in B-meson decays.

Furthermore, individual tracks and reconstructed vertices are subjected to constraints on their impact parameters with respect to the IP, reducing contributions from long-lived background particles and detector noise. These selections are designed to preserve an unbiased decay-time distribution while providing a clean input sample for multivariate background suppression and subsequent lifetime fitting.

The procedures described above yield a high-quality dataset of D^0 candidates with well-reconstructed kinematics and decay-time information. This dataset forms the foundation for the continuum suppression using machine learning techniques, which is the subject of the next section.

Chapter 4

Analysis Strategy and Multivariate Analysis

4.1 Overview of Analysis Strategy

The central objective of this thesis is to measure the lifetime of the neutral D^0 meson with high precision using data from the Belle II experiment. In addition to this primary physics goal, the analysis is designed to establish a modular, transparent, and reproducible framework that can be readily extended to lifetime measurements of other charm hadrons, such as D^+, D_S^+ and Λ_c^+. Emphasis is placed on maintaining consistency in signal selection, background suppression, and statistical modeling, ensuring that the methodology remains robust across different decay topologies and datasets.

A series of preliminary cuts can be performed during or just after the reconstruction process to enhance the performance of the sample of candidate events. These preliminary selections consist of kinematic cuts, vertex cuts, invariant mass windows,

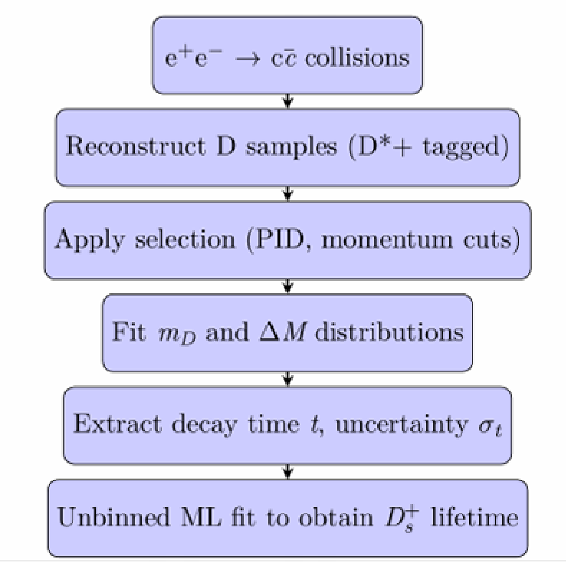

FIGURE 4.1: Analysis Workflow

and soft momentum cuts intended to mitigate the background due to the secondary production of charmed particles in B-meson decays. The goal at this point is to make rather loose selections in order not to alter the shape of the decay time distribution.

The dominant challenge in this analysis arises from the overwhelming presence of continuum background. Events originating from light-quark pair production ($e^+e^- \to q\bar{q}$ with q = u,d,s,c) far exceed the rate of genuine charmn meson decays and often mimic the kinematic properties of the signal, As these backgrounds cannot be efficiently suppressed using one-dimensional cuts, a multivariate analysis (MVA) approach is employed.

4.2 Multivariate Event Selection Strategy

Even for the most basic MC dataset, the invariant mass window around the nominal D^0 mass suffers severe contamination due to combinatorial background. Such background events come from accidental combinations of particles satisfying the kinematics of the decay, but not necessarily coming from real D^0 decays. Therefore, a selection solely based on the invariant mass variable is not enough to create a sample suitable for accurate lifetime measurements.

To cope with such a difficult problem, one can rely on further kinematic and geometric variables describing the decay topology, the production process, and the quality of the reconstructed vertex of the D^0 candidate. Together, such variables carry much more discriminating power compared to using each observable separately. That is why a multivariate analysis (MVA) technique should be used.

4.2.1 Choice of Multivariate Classifier

In the current investigation, FastBDT will be used as the main multivariate classifier. FastBDT is a gradient-boosted decision tree technique tailored for usage in high-energy physics, providing rapid training, minimal memory consumption, and good efficiency while dealing with large datasets containing highly correlated input parameters. In contrast to standard selection based on cuts, boosted decision trees can learn complex decision boundaries and discover the best combination of variables.

FastBDT is especially appropriate for this work because:

- its robustness against overtraining when properly tuned,
- its ability to handle mixed kinematic and geometric inputs,
- and its computational efficiency, which is critical when training and applying models across multiple decay channels.

Other alternative approaches that have been tested including Random Forest models and classifiers from the TMVA suite. Even though these techniques exhibit similar separation capabilities, FastBDT was selected as a benchmark model owing to its high speed, stability, and superior efficiency.

4.2.2 Input Variables for Signal-Background Separation

A wide set of candidate-level observables was explored to identify variables with strong discriminating power between signal and background. The most effective separation was achieved using a combination of the following key inputs:

- **Charm Flavour Tagging (CFT)** output: provides information related to the production and decay characteristics of charm mesons.
- **Candidate momentum in the center-of-mass (CMS)** frame: signal D^0 mesons tend to exhibit a harder momentum spectrum compared to combinatorial background.
- **Helicity angle**: encodes angular correlations of the decay products, which differ between true two-body decays and random track combinations.
- **Cosine of the angle between the reconstructed momentum vector and the vertex displacement vector**: serves as a powerful geometric consistency check, as genuine decays exhibit strong alignment between flight direction and momentum.

These variables, along with additional vertex-quality and topological observables, collectively enable a substantial enhancement in signal purity while retaining high efficiency.

4.2.3 Role of MVA in Lifetime Analysis

In the previous studies on the analysis of this problem, the output of the MVA was mainly employed as a rigid criterion for the suppression of the background, after which a lifetime fit was carried out using signal MC together with the randomly selected background events. Although this procedure is valuable for validating the algorithm, it fails to reproduce the actual situation that arises during data analysis.

In the current research, the purpose of the MVA goes beyond the mere suppression of the background. In fact, its output is applied to calculate the signal purity depending on the output of the MVA, thereby allowing one to optimize the sidebands in the invariant mass spectrum. The benefits of such an approach include:

- It avoids assumptions about the background composition.
- It allows the signal fraction entering the lifetime fit to be determined directly from the data.
- It provides a more realistic and robust framework for lifetime extraction, closely mirroring experimental analyses.

By incorporating the MVA-derived purity into the sideband optimization and subsequent mass and lifetime fits, the analysis achieves improved control over systematic effects arising from background modeling.

4.2.4 Analysis Workflow

The overall workflow of the event selection and lifetime analysis is summarized schematically in:

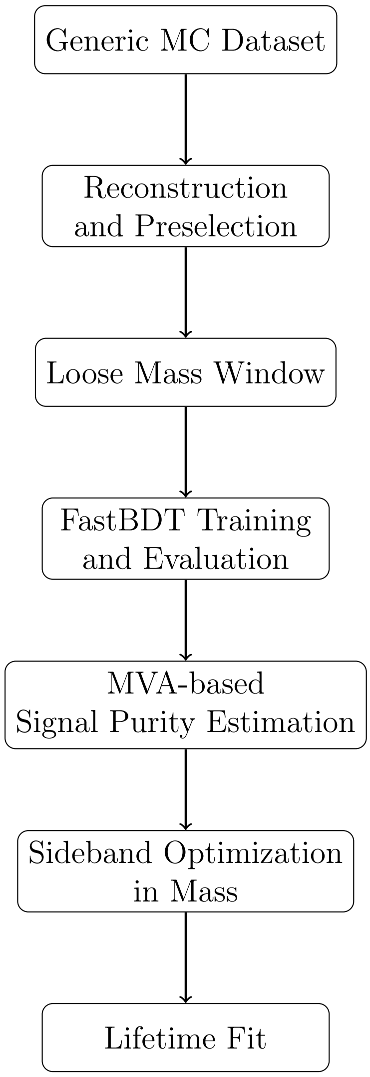

FIGURE 4.2: Schematic overview of the multivariate event selection and lifetime analysis workflow.

4.3 Training, Validation and Performance Evaluation of the MVA

This section explains the training process, validation methodology, and performance of the multivariate classifiers applied to event selection in this analysis. Following the motivation and variable selections presented in the previous section, the emphasis in this section is placed on the requirement for obtaining signal-background separation with good statistical and systematic properties.

In particular, the classification is done by means of an MVA, which is trained on simulated signal and background events. The samples are split into statistically independent training and test subsamples. Overtraining control, therefore, is available for such an approach. The optimal response of the classifier is obtained based on the figure of merit motivated by the physics of the problem to make sure that the final operating point of the classifier is appropriate for further mass and lifetime fits.

There are several approaches for checking and validating the MVA response and performance. These methods include overtraining studies through comparison of the responses for the training and testing data, receiver operating characteristic (ROC) curves, and ranking of the variables used to compute the classification function.

The rest of this section is structured as follows: first, the data set preparation and training settings are discussed, including the selected training/testing partition and optimization objectives. The topics then shift to over-training testing, classifier evaluation, and the physical meaning of the most influential inputs.

4.3.1 Dataset Preparation and Training Configuration

This multivariate discrimination technique employs MC samples containing both signals and backgrounds. The signals represent well-reconstructed events in which the D^0 meson decayed into one of the channels listed above. Backgrounds consist mostly of combinatorial and continuum events which passed the reconstruction-level selections. The advantage of using MC truth is the possibility of clear distinction between signal and background in the training process based on information contained in MC truth files.

At the beginning of the analysis, we employ loose baseline selections applied to both signal and background samples. These selections are characterized by wide mass windows, vertex requirement, and momentum cut-off. The purpose of employing baseline selection before training is not to optimize the efficiency and purity of the sample but to avoid the appearance of anomalous events and to minimize the computation time while keeping all the discriminatory power of the multivariate analysis method.

The available dataset is divided into two statistically independent subsets following an 80/20 split, with 80% of the events used for training and the remaining 20% reserved for testing and validation. This separation ensures that the performance of the classifier can be evaluated on data that were not used during the learning process, thereby providing a reliable assessment of its generalization capability. The training and test samples are drawn randomly from the same parent distribution to avoid kinematic or topological biases.

The classifier employed in this study is a FastBDT. This algorithm is chosen due to its computational efficiency, robustness against overtraining, and proven performance in high-energy physics applications involving large datasets and correlated input variables. FastBDT implements gradient boosting with optimized memory handling and fast inference, making it particularly well suited for iterative optimization studies such as figure-of-merit scans and sideband tuning.

An input variable list, which includes kinematic, geometrical, and event topology information, is provided to the classifier. The choice of the variables is motivated by physics arguments, previous research experience, and discriminatory capabilities of each observable to distinguish between signal and background processes. Each of the variables is carefully examined in both signal and background samples, and its distribution is verified against a test sample. The variables with problematic properties or significant mismodeling are removed from the list.

Training of the classifier is carried out using certain fixed hyperparameters, selected with discrimination capabilities and stability in mind. Instead of finding the optimal values for the hyperparameters in order to achieve best possible performance of the classifier, conservative values are used to avoid overtraining and allow for better reproduction of the classifier. The same training procedure and the same values for hyperparameters are used for all considered decays.

After completing the training process, the classifier output, henceforth called the MVA response, is calculated for both the training and the test sample. The MVA response acts as a continuous discriminant that is expected to have high values when the events are likely to be signals. Thresholding of the MVA response will be done after this point. It is kept as a floating variable for subsequent analyses such as overtraining studies, ROC studies, and figure-of-merit optimization.

This approach to training is an important basis for the performance studies presented in the following subsections. It ensures statistical independence between the training and testing samples as well as making sure that only the physical configuration was used.

4.3.2 Overtraining Checks and Model Validation

One of the most important criteria of applicability of any multivariate classifier for the precision measurement in high-energy physics is good ability to generalize. Overtraining may produce false improvement of classification efficiency at the training stage and worse results when tested on independent data. This leads to the bias in measurements of physics quantities, including purity of signal and lifetime distribution. Hence, a special validation is required to check on overtraining of the FastBDT classifier.

For this purpose, the distributions of FastBDT response in both training and test data sets are compared. After training the algorithm, the response is calculated in both training and test samples, and normalized distributions are built. If there was no overtraining, distributions for training and test data sets should have statistically consistent shapes, meaning that FastBDT learned physically distinct characteristics and did not memorize statistical fluctuations.

Concerning signal events, it can be seen that the distribution of the FastBDT response is characterized by a sharp maximum at large classifier scores, corresponding to the proper classification of real decays. As for background, its response distribution mostly takes place at low values of classifier scores with some smooth tail moving towards signal region. Importantly, there are no visible deformations and bumps in either distribution which might indicate an overtraining, as training and testing distributions coincide perfectly.

Apart from the comparison of shape distributions of classifier responses, it was also done the analysis of classifier stability by testing its response for different decay channels. Because the same training procedure and set of hyperparameters are used for all the channels considered, good stability of classifiers' response is expected for them. This expectation has been confirmed by performing the stability check: no anomalies for particular decay channels have been found. The only exception to this is the drop in efficiency in channels having neutral daughter particles, since it's not possible to exactly track neutral particle trajectories, simply from the very principles of a detector.

An additional validation procedure requires the check whether the output of the FastBDT classification is strongly correlated with the reconstructed mass of the D0 candidate. High correlations would introduce a strong shape deformation of the mass histogram after imposing the classifier cut, which would cause biases during the mass fit and purity evaluation procedure. As it was shown in the correlation analysis, even though there is no way to avoid weak correlations since both mass and kinematic consistency are physical observables, the FastBDT output is still well decorrelated from the mass inside the signal region.

This makes the classifier safe to use for further data selection before applying the mass fit. The robustness of the classifier and its lack of overtraining are especially crucial when performing the lifetime measurement. Since the distribution of decay times is rather sensitive to small deformations, a classifier-induced bias could directly affect the lifetime fit result.

First, we have below the difference in variable characteristics between signal and background events for the variables that were finally used in suppressing background events:

The overtraining plots for the machine learning model training and validation are also attached for a couple of the channels to demonstrate model efficiency, along with the corresponding classification results.

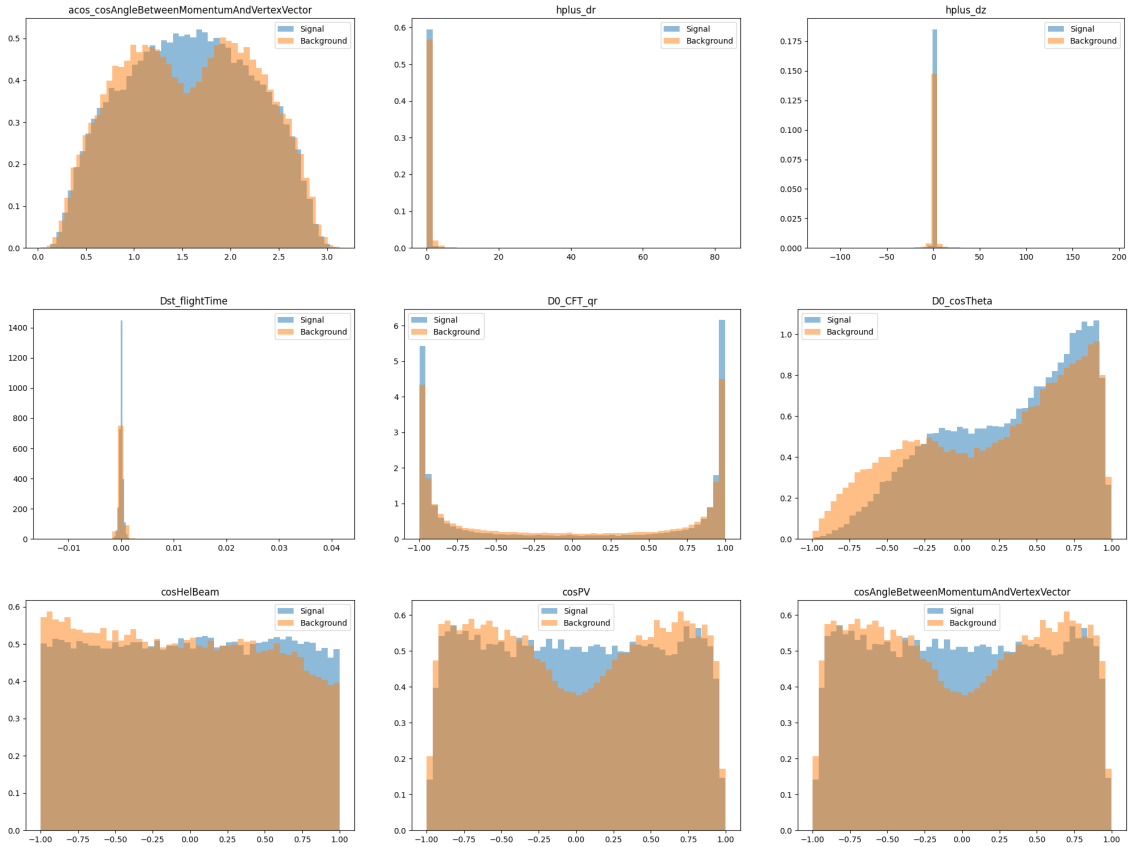

FIGURE 4.3: Distributions of representative kinematic and topological variables used as inputs to the FastBDT classifier.

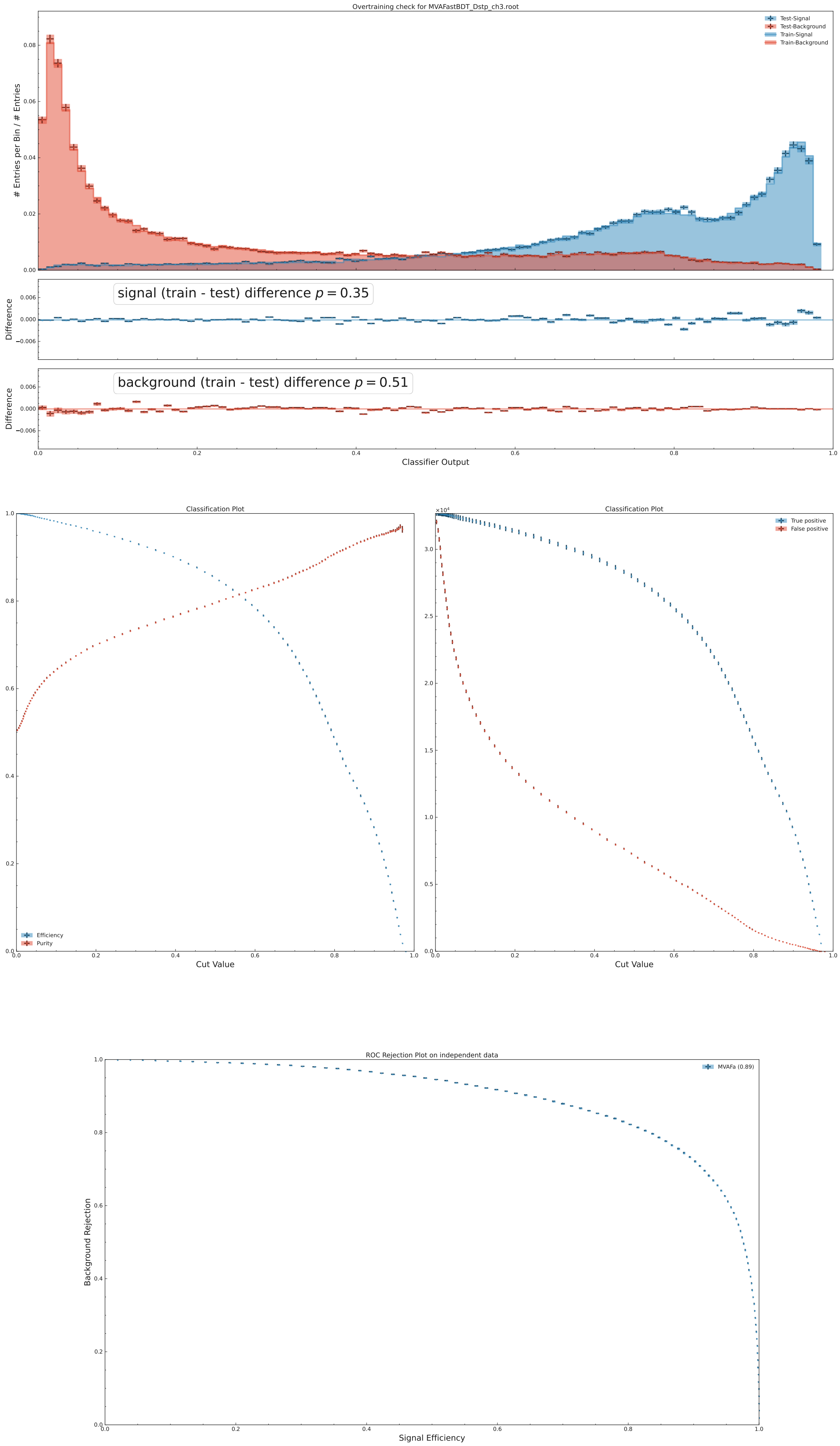

FIGURE 4.4: Performance diagnostics of the FastBDT classifier on Channel 3: (top to bottom) overtraining check, classifier response distribution, and receiver operating characteristic (ROC) curves evaluated on the test dataset.

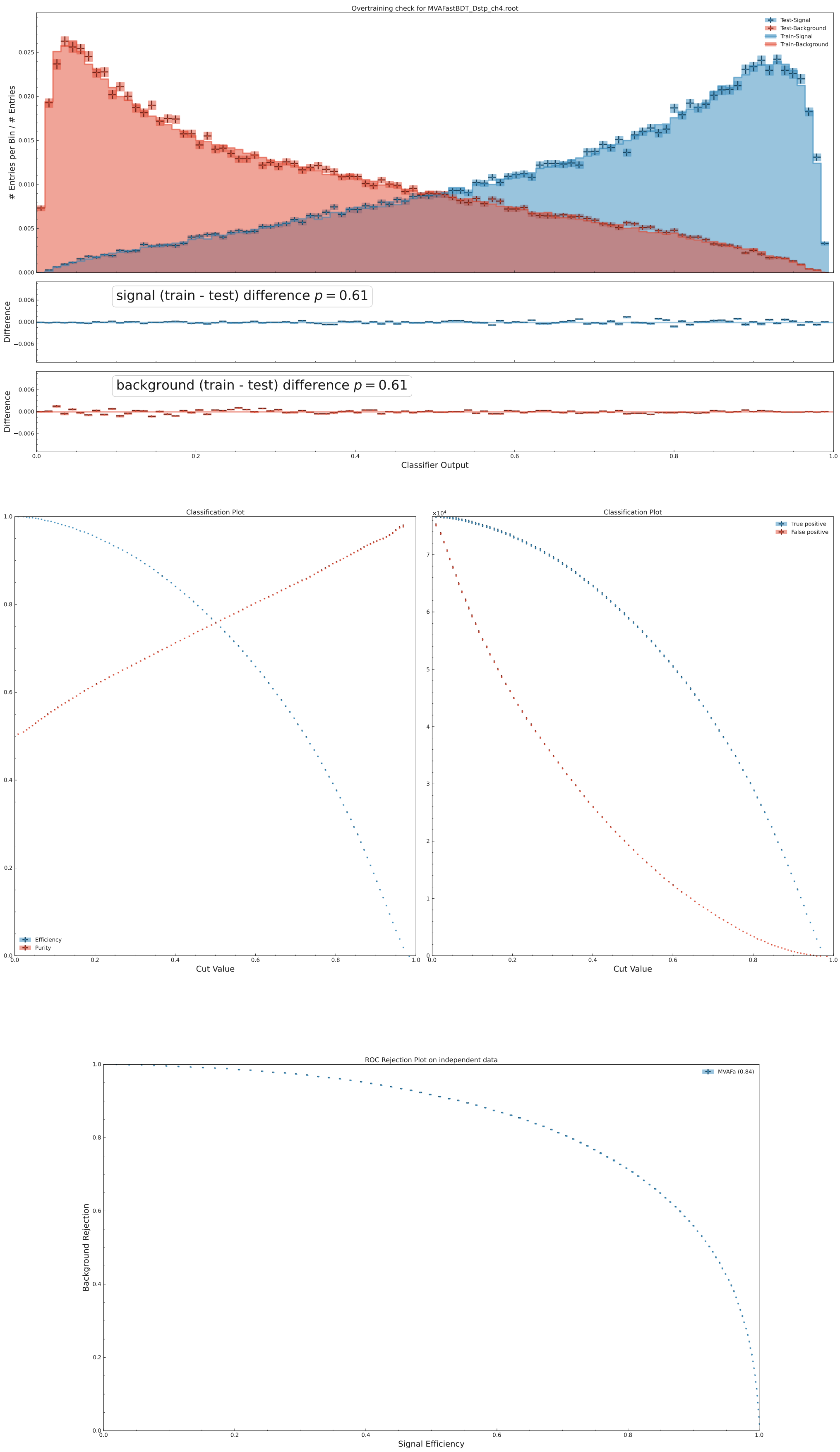

FIGURE 4.5: Performance diagnostics of the FastBDT classifier on Channel 4: (top to bottom) overtraining check, classifier response distribution, and receiver operating characteristic (ROC) curves evaluated on the test dataset.

4.3.3 Figure of Merit Optimization, Variable Importance and Correlation Studies

The performance of the classifier used in the precision measurement is not only dependent on the effectiveness of discrimination between signal and background, but also on the transformation of the classifier response to a physical event selection. For this measurement, the tuning of the working point for the multivariate classifier is carried out according to a certain Figure of Merit (FoM) criterion, while the internal structure of the classifier itself is studied by performing variable importance and correlation analyses.

4.3.3.1 FOM Optimization

Once the FastBDT classifier was trained, the performance of the classifier was studied as a function of a threshold on the score to find the best operating point. In order to do that, for all possible cuts in the classifier, the efficiency for the signal and background yields are determined based on two separate test samples that are statistically independent from each other. Then, a Figure of Merit (FoM), that is used to weigh signal efficiency versus background rejection, is computed.

The specific form of the FoM used in this analysis is defined as:

$$\mathrm{FoM} = \frac{S}{\sqrt{S+B}}$$

where:

- S is the number of signal events passing the BDT cut,
- B is the number of background events passing the same cut.

This formulation seeks to maximize the statistical significance of the signal under Poisson statistics and assumes that the background is not known with high precision. In cases where background estimation is robust and systematic uncertainties are low, a more sophisticated FoM incorporating uncertainties may be used, but for this study, the standard definition suffices.

Here, instead of maximizing signal acceptance, FoM has been constructed such that the optimal cut corresponds to having the highest sensitivity in the lifetime measurement. Background events can modify the shape of the decay time distribution and cause a bias in determining the lifetime. It is then preferable to have a signal sample with a relatively high purity despite losing some efficiency in accepting the signal events. Therefore, the optimal BDT cut is found where the FoM is maximized.

The chosen working point is then fixed and consistently used in the subsequent analysis steps, including the mass fit, determination of the sidebands, and lifetime determination.

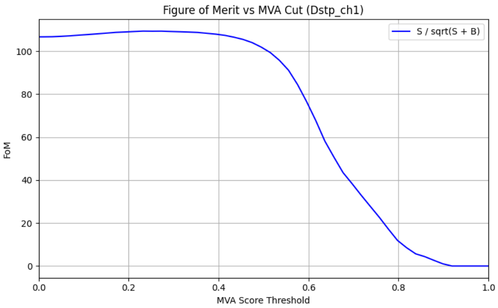

(a) Channel 1

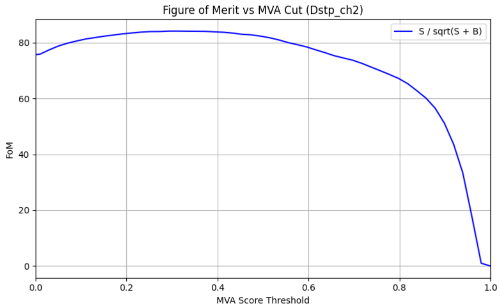

(b) Channel 2

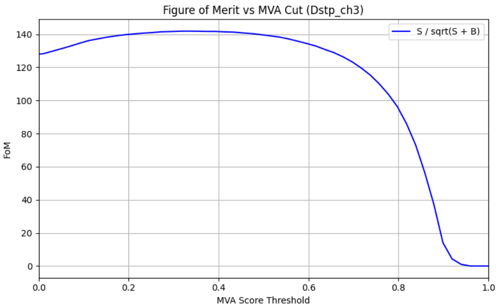

(c) Channel 3

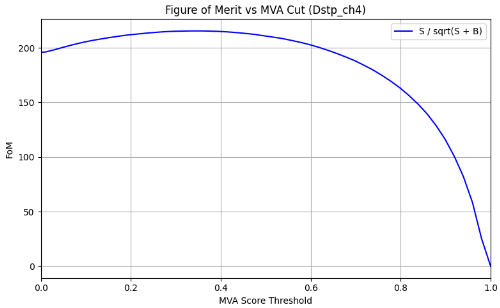

(d) Channel 4

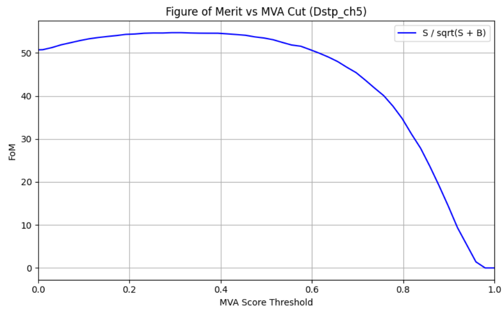

(e) Channel 5

FIGURE 4.6: Figure of Merit optimization curves for the five reconstructed D^0 decay channels. The optimal working point is chosen at the maximum of each curve.

4.3.3.2 Variable Importance

To gain insight into the physical features driving the classifier's decision-making, the relative importance of each input variable is evaluated. In FastBDT, variable importance is quantified based on the cumulative separation gain achieved by splits on a given variable across all trees in the ensemble. Variables with higher importance contribute more strongly to the discrimination between signal and background.

The most influential inputs are found to be those closely related to decay topology, vertex quality, and kinematic consistency with a promptly produced D^0 meson. These include quantities sensitive to the alignment between the reconstructed momentum and flight direction, the quality of the decay vertex fit, and global event properties indicative of charm production rather than continuum background.

For clarity and compactness in plots and tables, abbreviated variable names are used throughout the analysis. These correspond to the following full definitions:

- **Dst_c**: `Dst_cosHelDst1`
- **D0_ch**: `D0_chisq`
- **D0_p_**: `D0_p_CMS`
- **hplus**: `hplus_dr`
- **D0_CF**: `D0_CFT_qr`
- **D0_fl**: `D0_flightDistance`
- **D0_de**: `D0_decayangle0`

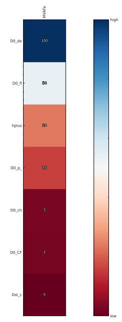

FIGURE 4.7: Variable Importance study

The prominence of these variables confirms that the classifier primarily exploits physically well-motivated observables, rather than artifacts of detector response or poorly understood correlations.

4.3.3.3 Correlation Studies

Apart from the variable importance, the pairwise correlations between the input variables are investigated independently for signal and background events. Correlations between different variables might lower the effective dimensionality of the variable space and might cause problems in case of an incorrect treatment.

According to the results previously shown, most of the variables with high importance show low correlations with each other, implying that they complement each other in the classifier. In cases where some of the variables are highly correlated, especially those related to the vertex properties, the findings are in agreement with the underlying physics laws, and the issue is correctly addressed due to the nature of the FastBDT tree-based algorithm.

This set of investigations confirms the robustness, interpretability, and reliability of the physics-based multivariate approach. Through the combination of the FoM

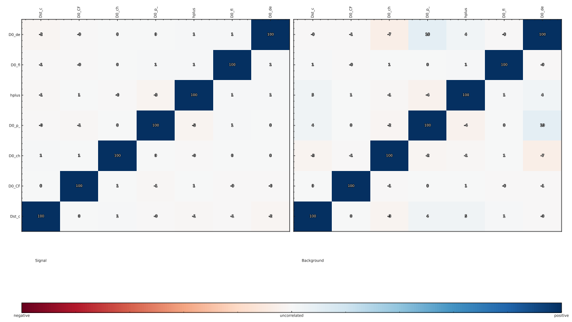

FIGURE 4.8: Correlation Plot

optimization procedure with the examination of the variable importance and their correlations, it is possible to find the most efficient configuration for the classifier.

4.4 Study of $K_S^0 \to \pi^+\pi^-$ Reconstruction Using Multivariate Techniques

The reconstruction of neutral long-lived particles provides a stringent test of vertexing and tracking performance, particularly in the presence of large combinatorial backgrounds. The decay

$$K_S^0 \to \pi^+\pi^-$$

is of special importance in charm and flavor physics analyses, but its identification is challenged by displaced decay topology, fake track combinations, and contamination from competing V^0 decays such as

$$\Lambda^0 \to p\pi^-$$

Traditional reconstruction strategies rely on a small set of topological variables, while more recent approaches employ multivariate classifiers to exploit correlations among a larger number of observables. This study builds upon earlier work [Ks

Finder] that introduced a neural-network-based K_S^0 selection ("nisKsFinder"), and adapts the core ideas to a FastBDT-based framework.

4.4.1 Conventional goodKs Selection Strategy

The standard goodKs method identifies K_S^0 candidates using a limited set of geometrical and kinematic variables designed to capture the essential features of V^0 decays. These variables reflect the following physical characteristics:

- The two daughter pions originate from a common displaced vertex.
- The K_S^0 decay vertex is spatially separated from the interaction point (IP).
- The reconstructed momentum of the K_S^0 points back toward its decay vertex.

Concretely, the goodKs selection uses four primary variables:

1. **Distance between the two daughter helices in the z-direction**, ensuring a common origin along the beam axis.
2. **Flight length in the transverse (x–y) plane**, exploiting the finite lifetime of the K_S.
3. **Angle between the K_S momentum in its rest frame and its direction in the laboratory frame**, probing decay topology consistency.
4. **Shorter distance between the interaction point and the daughter helices**, used to suppress prompt background combinations.

While these variables provide effective baseline discrimination, they do not fully exploit the available information, especially in regions where signal and background distributions overlap significantly.

4.4.2 Extended Variable Set and Multivariate Selection

To improve both purity and efficiency, the nisKsFinder approach augmented the goodKs variable set with additional kinematic and geometric observables. Motivated by this strategy, a similar but independent multivariate selection was implemented in this analysis using a FastBDT classifier.

In addition to the four goodKs variables, the following quantities were used as inputs:

- K_S **momentum**, sensitive to differences between signal and combinatorial background.
- **Longer distance between the IP and daughter helices**, complementary to the shorter-distance variable; background tends to cluster near small values, while genuine K_S candidates extend to larger distances.
- **Angle between the K_S momentum in the laboratory frame and the pion momentum in the K_S rest frame**, which shows distinct behavior for misidentified daughter particles.

The classifier achieved strong separation power. In particular, the angular and flight-distance variables proved highly effective in suppressing backgrounds arising from random track combinations and from baryonic decays.

4.4.3 Performance and Background Suppression

The multivariate selection demonstrates excellent discrimination between genuine K_S decay and background, even in the presence of significant contamination from:

$$Lambda^0 \to p\pi^-$$

which closely mimics the V^0 topology when the proton is misidentified as a pion.The strong performance of the FastBDT classifier highlights two key observations:

- Correlations among topological variables play a crucial role in separating signal from background and are not fully captured by cut-based selections.
- Even without explicit tracker hit information, high purity and efficiency can be achieved by exploiting decay geometry and kinematics alone.

This study confirms that multivariate approaches provide a substantial improvement over traditional goodKs methods and validates the use of FastBDT-based classifiers for neutral V^0 reconstruction in high-background environments. Furthermore, it opens a door to the possibility of using multiple MVA analyses, as will be discussed in a forthcoming chapter.

The results from the training and validation of FastBDT on this model are attached below:

Alongside this, at different candidate mass ranges, the models showed varying performances, with varying best cuts and purity vs. efficiency graphs, which has been shown below:

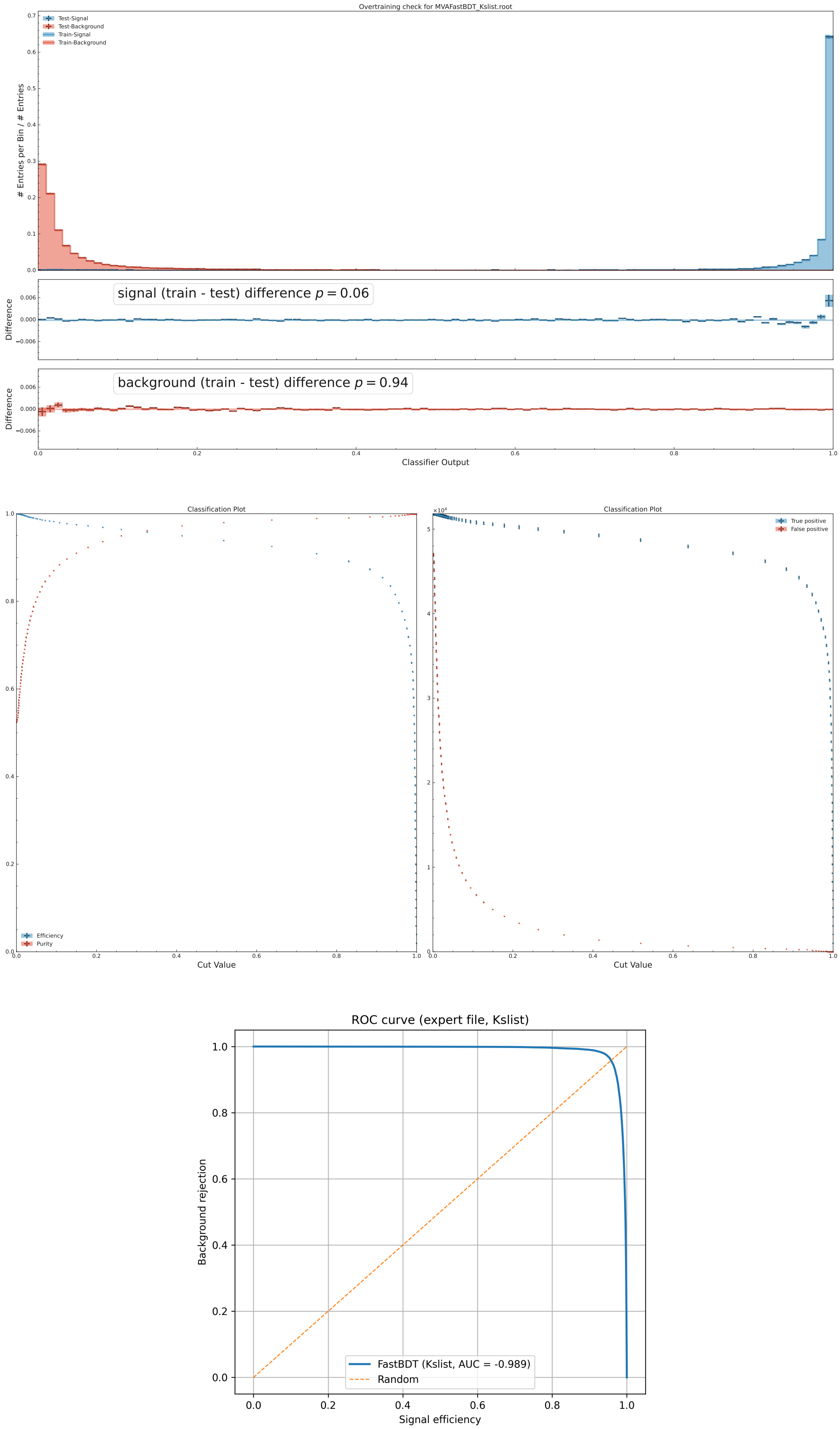

FIGURE 4.9: Performance diagnostics of the FastBDT classifier on Ks-Decay: (top to bottom) overtraining check, classifier response distribution, and receiver operating characteristic (ROC) curves evaluated on the test dataset.

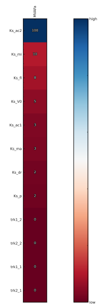

FIGURE 4.10: Importance

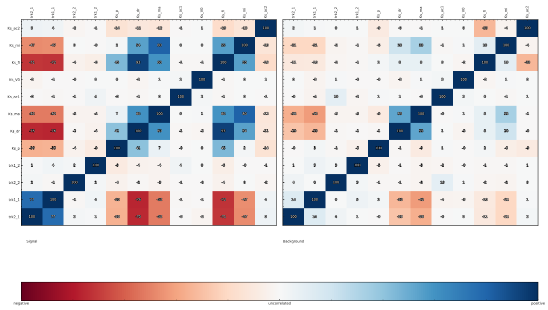

FIGURE 4.11: Correlation

FIGURE 4.12: Variable Statistics

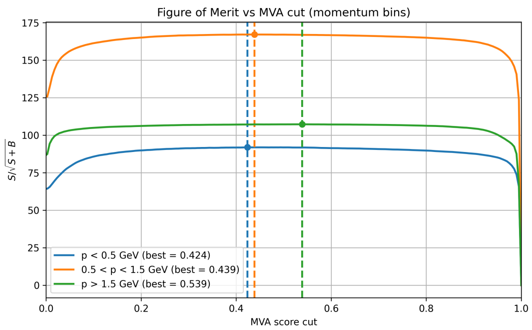

FIGURE 4.13: FOM

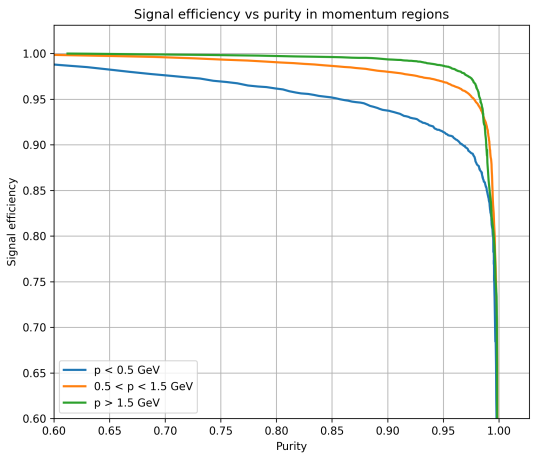

FIGURE 4.14: Purity vs. Efficiency

FIGURE 4.15: Dependance on candidate Momentum bins

Chapter 5

Lifetime Fitting Procedure

5.1 Introduction

The calculation of the D^0 meson lifetime is the last step and at the same time the most sensitive procedure in this research. Although previous chapters describe all the methods needed for selecting a pure signal sample, the lifetime determination requires a precise mathematical method of studying the decay time distribution of signal and background events. This chapter will discuss in detail the approach used in the measurement of the lifetime, beginning from modeling the influence of various resolutions on the experiment results.

Instead of simplifying the problem of lifetime measurement and assuming that it follows an exponential distribution, a realistic experiment requires consideration of additional factors such as vertex resolution, uncertainty in decay time calculations, residual combinatorial background, and distortions caused by applying the selection algorithm. The analysis of lifetime can be divided into a series of interconnected procedures, each providing some important information for building the likelihood function.

The procedure begins with the characterization of the decay time resolution function, which accounts for the smearing introduced by tracking and vertex reconstruction uncertainties. This resolution model is essential for relating the true physical decay time to the reconstructed observable.

Following this, a mass fit of the reconstructed D^0 candidates is performed to separate signal from background in invariant mass space. The outcome of this fit is used to define the signal region and to estimate the signal purity, which plays a central role in constraining the relative contributions of signal and background in the lifetime fit.

In parallel, the background decay time distribution is modeled using data-driven techniques. This includes fitting sideband regions in the invariant mass spectrum, which provide an empirical description of the combinatorial background without relying on simulation assumptions.

An important part of this process includes the test of sideband background shape versus background in the signal region. The purpose of this test is to ensure that the sideband background modeling represents the background below the signal resonance, and minimize the bias induced due to possible mass-time correlations.

All pieces discussed above are merged in a global unbinned maximum likelihood fit, where the signal decay function, resolution effects, and background functions are taken into account. The value of the D^0 lifetime is determined as the main quantity of interest during this process.

The structure of this chapter follows this logic, starting with the discussion on resolution effects, proceeding to mass reconstruction and signal extraction, background estimation, and finishing with the description of the overall lifetime fitting procedure.

5.2 Decay Time Resolution Function

The accuracy of the lifetime extraction relies critically on a precise characterization of the decay time resolution. In an ideal detector, the decay time distribution of a long-lived particle would follow a pure exponential form. In practice, however, finite tracking precision, vertex reconstruction uncertainties, and detector geometry effects smear the true decay time. As a result, the observed decay time distribution corresponds to a convolution of the physical decay model with an experimental resolution function. An accurate description of this resolution is therefore essential for an unbiased lifetime measurement.

To construct the resolution model, signal Monte Carlo (MC) events passing the full analysis selection were used. For each event, the difference between the reconstructed decay time and the true MC decay time was computed and used as a proxy for the detector resolution on an event-by-event basis. This quantity is defined as:

$$\Delta t = t_{reco} - t_{MC}$$

where t_{reco} is the reconstructed decay time obtained from vertex fitting, and t_{MC} is the true decay time provided by the generator-level information. The resulting Δt distribution encapsulates the combined effects of track parameter resolution, vertex fitting performance, and detector alignment.

Several functional forms were investigated to model the Δt distribution. These include:

- a single Gaussian model,
- a double Gaussian model, consisting of a narrow core component and a broader tail component,
- a triple Gaussian model, incorporating one core and two tail components.

The single Gaussian model was found to be insufficient in describing the non-Gaussian tails present in the distribution, particularly those arising from poorly reconstructed vertices or detector edge effects. While the double Gaussian model provided an improved description, it did not fully capture the asymmetry and extended tails observed in the data. The triple Gaussian model offered the best balance between descriptive power and fit stability, accurately modeling both the narrow central peak and the broader tails of the distribution.

The resolution function is therefore parameterized as a weighted sum of three Gaussian components, each with its own width and relative fraction. The parameters of this model—namely the widths and fractional contributions of the three Gaussian components—were determined from a fit to the Δt distribution in signal MC and subsequently fixed for use in the lifetime fitting procedure.

Fixing the resolution parameters ensures that the lifetime fit remains stable and is not driven by statistical fluctuations in the decay time distribution. This approach also prevents strong correlations between resolution parameters and the lifetime parameter itself. The validated resolution model is then convolved with the physical decay time probability density function in the final lifetime fit, as previously described.

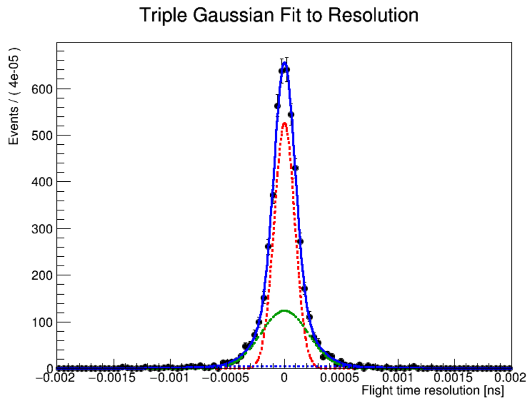

FIGURE 5.1: Resolution fit with triple gaussian

An example of the fitted decay time resolution distribution using the triple Gaussian model is shown below. The model provides an excellent description of the data across the full range of Δt, including both the core region and the non-Gaussian tails.

5.3 Invariant Mass Fit and Signal Purity Determination

The measurement of the lifetime of the D^0 meson depends on being applied to a pure sample of signal events. However, even after selecting the appropriate signal candidates using reconstruction level cuts and multivariate classifications, there will be a remaining contamination by combinatorial backgrounds. In order to measure the lifetime of D^0 mesons without introducing bias into the time distribution, one needs to discriminate the background from the signal and estimate their number.

This discrimination is performed using a fit in the space of the invariant mass of the reconstructed D^0 candidates. This method utilizes the fact that properly reconstructed signal decays result in a sharp peak close to the D^0 mass, whereas the combinatorial background forms a broad smooth distribution.

The distribution of the signal peak is described by the probability density function based on the Gaussian distribution, taking into account the impact of the detector resolution on the reconstructed mass. When there are small asymmetries or deviations from the Gaussian distribution in the tail, it is possible to describe the peak region with an extended Gaussian distribution.

The background contribution is estimated using an empirical function that depends on the order of the polynomial, usually first or second order (in this case second), to avoid any additional structure.

After fitting the distribution of the reconstructed mass with both components, the following are obtained:

1. Signal region definition, and
2. Estimation of signal purity within that region.

This is done rigorously (i.e., transferable to a real analysis) by using the MVA score and knowledge of a best cut to assign signal truth values to events. The signal region is defined around the fitted D^0 mass peak, typically as a symmetric window around the mean value. In this analysis, a window corresponding to approximately 3σ of the fitted Gaussian width is used. This choice ensures that the majority of true signal events are retained while significantly reducing the contribution from combinatorial background.

Within this signal window, the signal purity is determined from the fitted signal and background yields. The purity is defined as

$$P = \frac{N_{sig}}{N_{sig} + N_{bkg}}$$

Where N_{sig} and N_{bkg} are the signal and background yields obtained from the invariant mass fit within the selected region. This purity plays a central role in the subsequent lifetime fit, as it constrains the relative weight of signal and background components in the decay time likelihood model.

In addition to defining the signal region, the mass fit also provides an important cross-check of the reconstruction quality across different decay channels. Consistency in the fitted peak position and width confirms the stability of the detector response and ensures that no channel-specific biases are introduced at the reconstruction stage.

The fitted mass distribution demonstrates a clear separation between signal and background components, with a well-defined peak corresponding to true D^0 decays. The quality of the fit validates the choice of selection criteria and confirms that the multivariate classifier can accurately model signal and background probability distribution functions accurately in the subsequent analyses, instead of just eliminating background as was done in previous iterations.

The invariant mass fits used for signal yield extraction are shown in Figure 5.2.

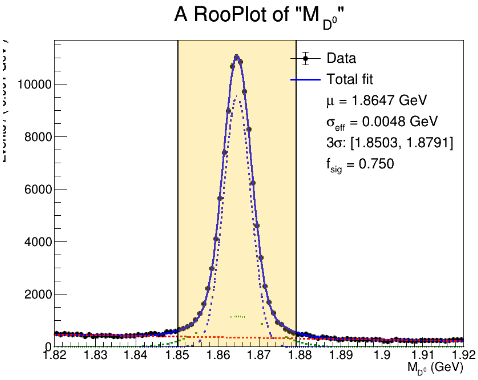

FIGURE 5.2: Channel 1

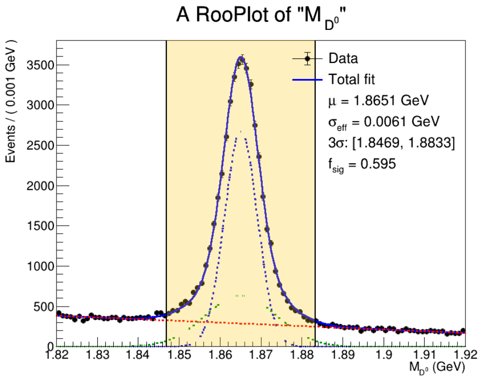

FIGURE 5.3: Channel 2

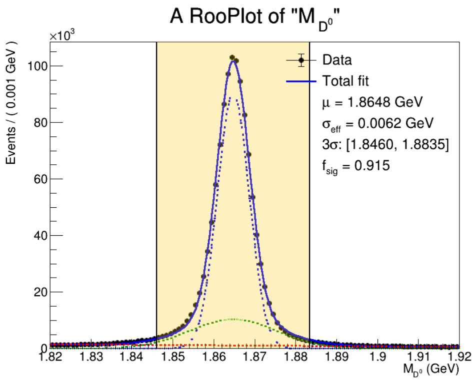

FIGURE 5.4: Channel 3

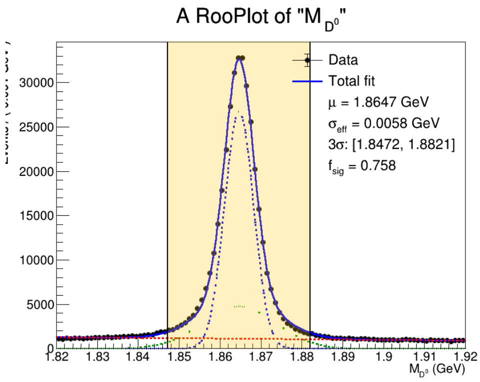

FIGURE 5.5: Channel 4

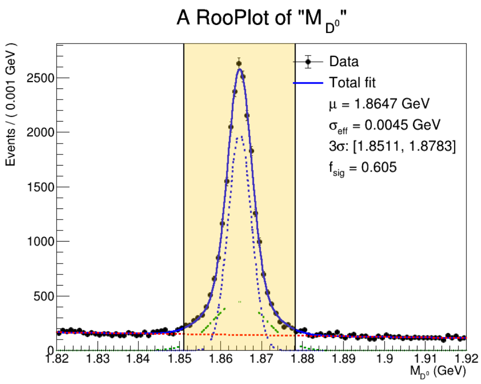

FIGURE 5.6: Channel 5

FIGURE 5.7: Invariant mass distributions and fitted signal + background components across the five D^0 decay channels.

The results of the mass fit are:

Channel	**Mean (GeV)**	**Eff. Sigma (GeV)**	**Purity ($\pm 3\sigma$)**
Dstp_ch1	1.86469	0.00489	75%
Dstp_ch2	1.86501	0.00658	59.5%
Dstp_ch3	1.86485	0.00620	91.5%
Dstp_ch4	1.86466	0.00568	75.8%
Dstp_ch5	1.86465	0.00475	60.5%

Table 5.1: Mass fit results for each channel.

5.4 Background Modeling and Sideband Validation

A reliable extraction of the D^0 meson lifetime requires an accurate description of the residual background present in the selected dataset. Even after applying multivariate selection criteria and restricting candidates to the signal mass window, a non-negligible fraction of combinatorial background remains. This background can distort the decay time distribution and introduce biases if not properly modeled.

To address this, a data-driven approach is adopted in which the background decay time distribution is extracted from invariant mass sidebands. The sideband regions are defined as mass intervals away from the D^0 signal peak, chosen such that they are dominated by combinatorial background while minimizing signal contamination. These regions provide an empirical representation of the background under the assumption that the decay time properties of combinatorial background are approximately independent of invariant mass.

The validity of this assumption is explicitly tested by comparing the decay time distributions of events in the sideband regions with those of background events within the signal region. The signal region is defined as a window around the fitted

D^0 mass peak, typically corresponding to 3σ of the mass resolution obtained from the invariant mass fit described in Section 5.3.

5.4.1 Sideband Construction

The sideband regions are constructed symmetrically around the signal peak, sufficiently far from the central mass region to suppress signal leakage. These regions are selected such that:

- They contain predominantly combinatorial background,
- They preserve similar kinematic and event-level characteristics as the signal region background,
- They maintain adequate statistical power for fitting the background decay time distribution.

Therefore, the signal region is defined as:

$$m \in [\mu_{M,D^0} - 3\sigma_{M,D^0}, \mu_{M,D^0} + 3\sigma_{M,D^0}]$$

The Sideband region is then correspondingly defined as:

$$m \in [\mu_{M,D^0} - 3\sigma_{M,D^0} - 0.2GeV, \mu_{M,D^0} - 3\sigma_{M,D^0}] \cup [\mu_{M,D^0} + 3\sigma_{M,D^0}, \mu_{M,D^0} + 3\sigma_{M,D^0} + 0.2GeV]$$

This ensures a clean separation between signal-dominated and background-dominated regions, while also only filtering for specific confounding background.

5.4.2 Background Decay Time Modeling

The decay time distribution of sideband events is used to construct an empirical probability density function (PDF) for the background component. Unlike signal decays, which follow an exponential decay law convolved with the detector resolution, background events exhibit no intrinsic lifetime structure. Instead, their distribution arises from random track combinations and misreconstructed vertices.

As a result, background decay time distributions are typically modelled using flexible functional forms such as gaussians (single, double or triple), Johnson's SU, a sum of exponential functions etc. For this analysis, it was found that a triple gaussian convolved on an exponential function gave the best fit and was used as the background template in the final likelihood fit.

The resultant fits are shown below:

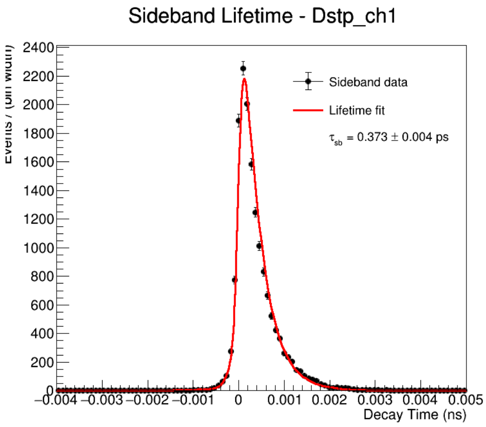

FIGURE 5.8: Channel 1

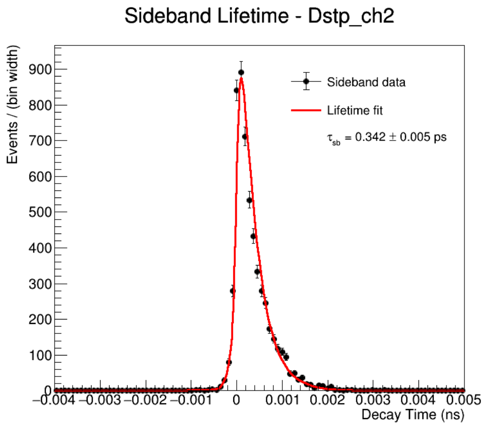

FIGURE 5.9: Channel 2

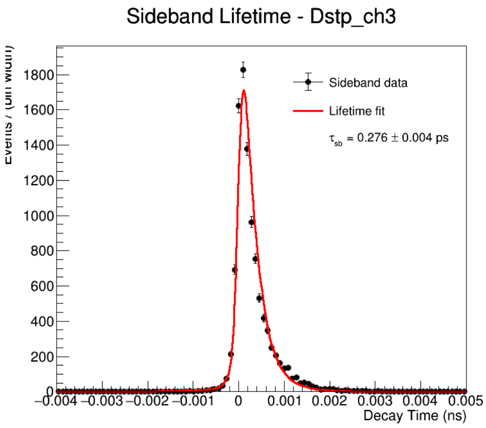

FIGURE 5.10: Channel 3

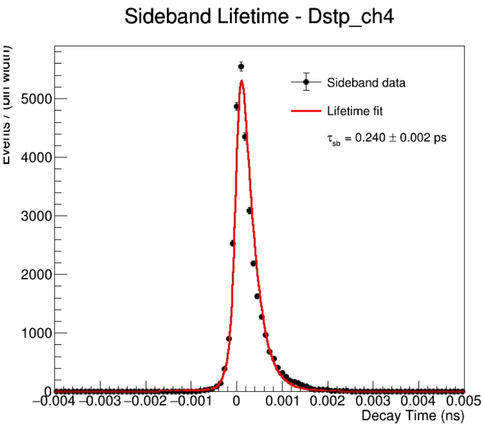

FIGURE 5.11: Channel 4

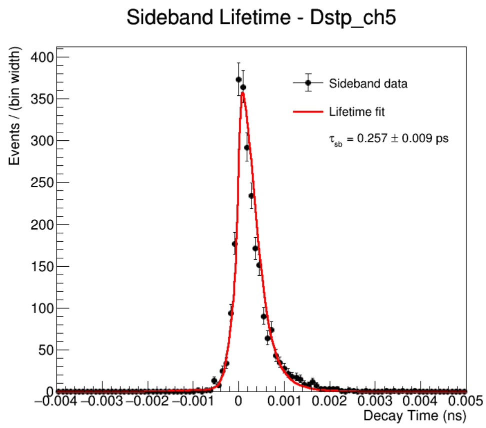

FIGURE 5.12: Channel 5

FIGURE 5.13: Sideband Lifetime fits

5.4.3 Validation Against Signal Region Background

A crucial test of this analysis method comes in the comparision of sideband background shapes to signal region background shapes. The efficacy of this method rests on the strength of the assumption that the background lifetimes are uniform across both signal and sideband regions. To verify this, a single plot containing all the background events was created with different colouring for the two regions, and the results show high correlation between both distributions.

The plots are attached below:

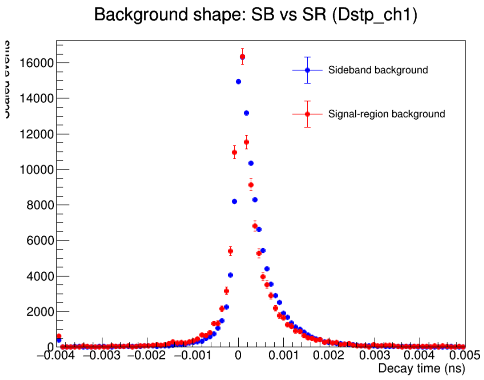

FIGURE 5.14: Channel 1

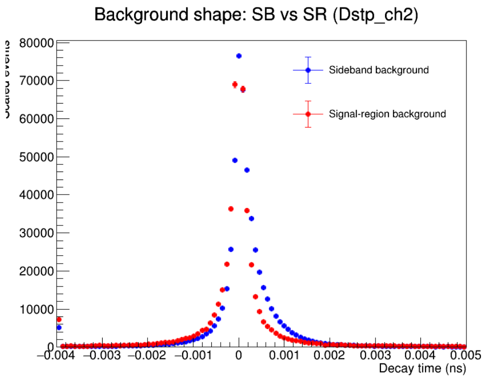

FIGURE 5.15: Channel 2

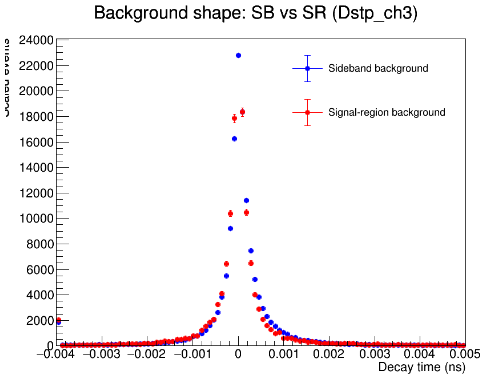

FIGURE 5.16: Channel 3

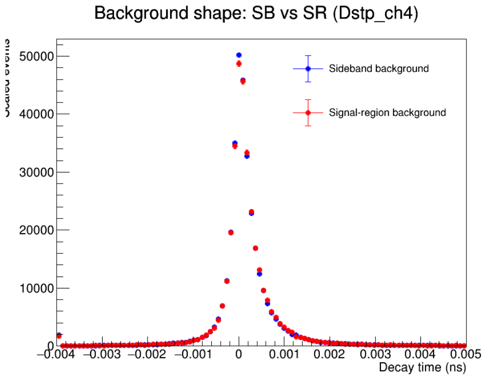

FIGURE 5.17: Channel 4

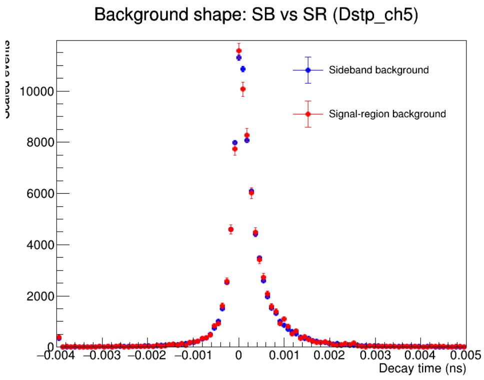

FIGURE 5.18: Channel 5

FIGURE 5.19: Sideband Lifetime fits

5.5 Combined Unbinned Maximum Likelihood Lifetime Fit

The final step in the analysis is the determination of the D^0 lifetime from an unbinned maximum likelihood fit to the decay time distribution. This step forms the conclusion of the complete analysis process, which involves incorporating all relevant information obtained throughout the reconstruction and selection processes, including the multivariate selection procedure, invariant mass fits, and the background model.

Each decay mode is fitted separately by means of the RooFit software suite included in the ROOT system. RooFit offers a powerful platform for the definition of composite probability density functions (PDFs) and their subsequent maximum likelihood analysis. The ultimate objective of the fit is to determine the lifetime parameter τ of the D0 meson from its decay time distribution.

5.5.1 Signal Decay Time model

The decay of a free D^0 meson is governed by an exponential law:

$$f(t') = \frac{1}{\tau} e^{-t'/\tau}$$

where t' is the true proper decay time and τ is the lifetime to be measured.

However, the experimentally reconstructed decay time t differs from the true decay time due to finite detector resolution effects, including vertex reconstruction uncertainties, track parameter smearing, and alignment effects. To model this, the observed signal probability density is constructed as a convolution of the exponential decay law with a resolution function:

$$P_{\text{sig}}(t^i|\tau, \sigma_t^i) = \frac{1}{\tau} \int e^{-t'/\tau} R(t^i - t'; \mu, s, \sigma_t^i)\, dt'$$

where:

- t_i is the reconstructed decay time for event i,
- σ_{t_i} is the per-event decay time uncertainty,
- R(Δt) is the detector resolution function.

The resolution function R is modeled as a **triple Gaussian**, defined as:

$$R(\Delta t) = \sum_{k=1}^{3} f_k \cdot G(\Delta t; \mu, \sigma_k \sigma_{t_i})$$

, where:

- f_k are the fractional contributions (with $\sum f_k = 1$),
- σ_k are scale factors applied to the per-event uncertainty,
- μ is a common mean

The parameters of this resolution function were fitted previously, but are fit once again in the total lifetime fit analysis.

5.5.2 Background Decay Time Model (Sideband-Constrained)

Unlike signal decays, background events do not follow a physical exponential decay law. Instead, they arise from random track combinations, misreconstructed vertices, and partially reconstructed charm decays.

In this analysis, the background decay time distribution is modeled using a data-driven sideband approach, as described in Section 5.3. The background PDF is obtained by fitting the decay time distribution of events in the invariant mass side-bands, which are dominated by combinatorial background.

The resulting background model is therefore:

$$P_{bkg}(t) = P_{sideband}(t)$$

, where $P_{sideband}(t)$ is the empirically extracted pdf describing the decay time structure of background events.

This approach removes reliance on assumptions such as prompt-only background behavior and ensures that any non-trivial structure in the background decay time distribution is directly captured from data.

5.5.3 Construction of the Full Likelihood

The full probability density function for each event is constructed as a weighted sum of signal and background contributions:

$$P(t_i) = f_{sig} \cdot P_{sig}(t_i|\tau, \sigma_{t_i}) + (1 - f_{sig}) \cdot P_{bkg}(t_i)$$

,

where:

- f_{sig} is the signal fraction obtained from the invariant mass fit,
- P_{sig} is the resolution-convolved exponential signal model,
- P_{bkg} is the sideband-derived background PDF.

The total likelihood for all N events is then given by:

$$L(\tau) = \prod_{i=1}^{N} P(t_i)$$

.

In practice, the logarithm of this likelihood is minimized, which is numerically optimized using RooFit's minimization algorithm.

5.5.4 Channel-Wise Fitting Strategy

The lifetime fit is performed independently for each of the five D^0 decay channels. This allows for:

- validation of consistency across decay modes,
- identification of channel-dependent systematic effects,
- cross-checks of reconstruction stability.

Each channel uses:

- its own signal fraction f_{sig}

- its own mass-defined signal region,
- a common resolution model derived from signal MC,
- a shared methodology for background modeling via sidebands.

This modular structure ensures that the measurement is both robust and internally consistent.

The lifetime plots are attached below:

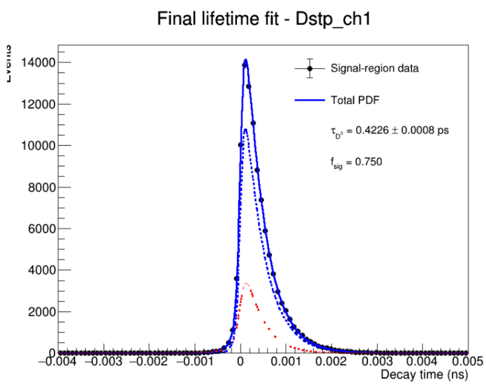

FIGURE 5.20: Channel 1

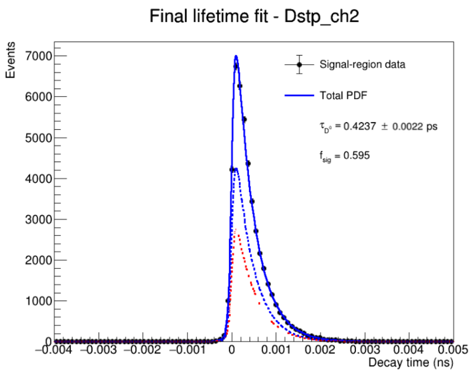

FIGURE 5.21: Channel 2

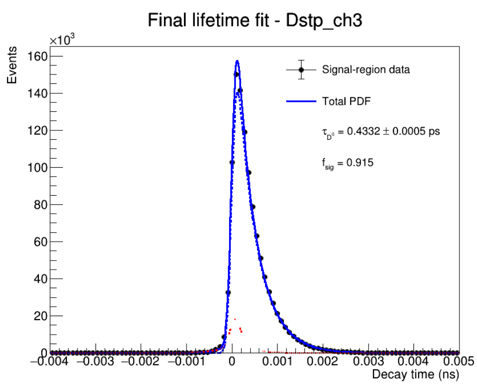

FIGURE 5.22: Channel 3

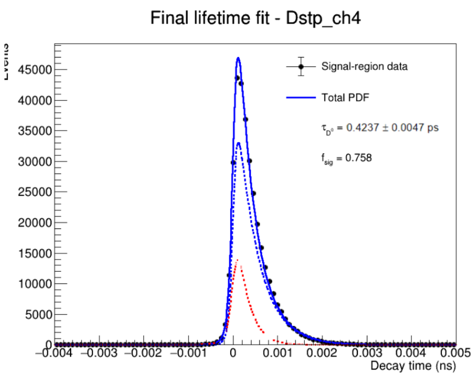

FIGURE 5.23: Channel 4

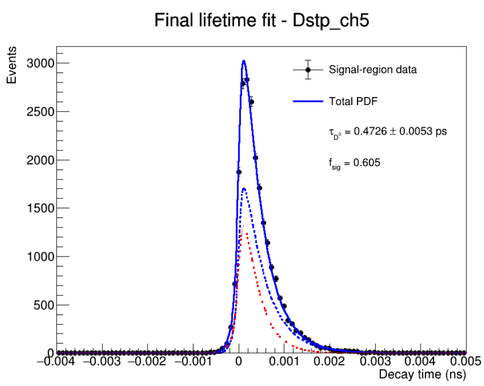

FIGURE 5.24: Channel 5

FIGURE 5.25: D^0 Lifetime fits

The final lifetime results, along with the current PDG results are shown in the table below:

Channel	**Lifetime (ps)**	**Error (ps)**
Dstp_ch1	0.4226	0.0008
Dstp_ch2	0.4237	0.0022
Dstp_ch3	0.4332	0.0005
Dstp_ch4	0.4237	0.0047
Dstp_ch5	0.4726	0.0053
PDG	0.4203	0.0010

Table 5.2: Lifetime fit results with associated errors for each channel.

Chapter 6

Conclusions, Discussions and Future Work

6.1 Conclusion

This thesis presented a complete framework for the measurement of the D^0 meson lifetime using Belle II Monte Carlo data. The analysis was designed to be modular, data-driven, and extendable to future charm physics studies, with particular emphasis on robust signal selection, background suppression, and statistically sound lifetime extraction.

Starting from a large generic MC dataset, five distinct D^0 decay channels were reconstructed and subjected to a consistent selection strategy. The reconstruction pipeline incorporated standard Belle II event-level filters, particle identification, vertex fitting, and kinematic constraints to ensure high-quality candidate selection.

To address the significant combinatorial background present even near the signal mass region, a multivariate approach based on FastBDT was employed. This allowed for efficient separation of signal-like and background-like events using a combination of kinematic, geometric, and event-shape variables. The classifier significantly improved the purity of the selected sample compared to traditional cut-based approaches.

Signal yields and purities were extracted through invariant mass fits performed independently for each decay channel. These results were used to define a well-controlled signal region and to quantify background contributions entering the lifetime fit.

A dedicated resolution model was constructed using signal Monte Carlo, where the distribution of $t_{reco} - t_{MC}$ was studied. A triple Gaussian parameterization was found to best describe the detector resolution and was subsequently fixed in the final lifetime fit.

Background contributions were modeled using a data-driven sideband technique, ensuring that the decay time structure of combinatorial background was directly extracted from data rather than relying on simulation assumptions. This provided a robust and minimally model-dependent description of the background component.

Finally, an unbinned maximum likelihood fit was performed to extract the D^0 lifetime. The fit combined:

- an exponential decay model for the signal,
- convolution with the resolution function,
- and a sideband-derived background PDF,
- with signal fractions constrained from the mass fits.

The consistency of results across all decay channels demonstrates the stability and reliability of the analysis framework.

6.2 Discussion

The results of this analysis highlight the importance of a fully integrated approach to precision lifetime measurements in modern flavor physics experiments. In particular, the combination of multivariate event selection and data-driven background modeling provides a significant improvement over traditional cut-based or simulation-dependent methods.

The FastBDT classifier proved to be a powerful tool for suppressing continuum background, especially in regions where kinematic overlap between signal and background is significant. The use of physically motivated input variables ensured that the model remained interpretable and robust, rather than purely empirical.

The adoption of sideband-based background modeling represents a key strength of this analysis. By extracting the background decay time distribution directly from data, the analysis avoids potential biases arising from simulation mismodeling or assumptions about promptness. The validation of sideband representativeness further strengthens the credibility of the lifetime fit.

The resolution modeling using a triple Gaussian function captures both core and non-Gaussian contributions to detector smearing, ensuring that the lifetime extraction is not biased by simplified assumptions. Fixing these parameters based on Monte Carlo studies stabilizes the fit and reduces correlations with the physics parameter of interest.

We see a significant improvement in lifetime uncertainties over PDG accepted values due to the powerful suppression granted by the well trained FastBDT models. The increased uncertainties in channels 4 and 5 occur as a result of background contamination as a result of one of the daughter particles (K_S) being a neutral particle.

Overall, the agreement and consistency across multiple decay channels suggest that the analysis framework is both robust and scalable. The methodology is directly applicable to other charm hadrons such as $^+$,D_s^+, Λ_c^+ and can be extended to larger datasets expected from future Belle II data-taking periods.

6.3 Future Work

While the current analysis provides a complete and self-consistent measurement framework, several extensions can further improve both precision and physics reach.

A natural next step is the application of this framework to real Belle II data, where additional detector effects and systematic uncertainties will become more relevant. This includes the incorporation of data-driven calibration techniques for vertex resolution and improved modeling of detector alignment effects.

The multivariate selection strategy can also be further enhanced. More advanced machine learning approaches such as deep neural networks or gradient-boosted ensembles with hyperparameter optimization may offer improved separation power, particularly in challenging decay channels with neutral particles or higher combinatorial backgrounds.

On the statistical side, a simultaneous fit across all decay channels could be implemented to extract a combined lifetime value with reduced statistical uncertainty.

This would also allow for a more systematic treatment of correlated uncertainties between channels.

In addition, a full systematic uncertainty study should be performed, including variations in:

- resolution model parameterization,
- background PDF choice,
- signal region definition,
- and selection criteria.

Specifically, there is potential in uniting the K_S study conducted alongside the main $D0$ lifetime project around which this thesis centers. As previously discussed, the presence of a neutral particle poses a large challenge in accurate background suppression. However, since the K_S study found a way to accurately reconstruct a neutral particle based on it's charged daughter particles, a composite MVA analysis can be conducted. If all candidate reconstructions also included granddaughter particle information, the K_S model could be applied to the daughter candidates and only a concurrent agreement in both models would imply a signal event, greatly boosting the background suppression in these analyses. This is supported by the fact that K_S primarily has only 2 decay modes, and $K_S \to \pi^+\pi^-$ is the only one which can be reconstructed as the other mode generates two neutral pions.

Finally, the techniques developed in this thesis—particularly the sideband-driven background modeling and multivariate selection framework—can be extended to other charm and heavy-flavor systems. This opens the possibility of precision measurements in related decay modes and contributes to broader tests of Heavy Quark Expansion (HQE) predictions in the charm sector

References

[1] R. J. Morrison and M.S. Witherell, "Annu. Rev. Nucl. Part. Sci." **39**, 183 (1989).

[2] T. E. Browder, K. Honscheid, and D. Pedrini, "Annu. Rev. Nucl. Part. Sci." **46**, 395 (1996).

[3] A. Lenz, "Int. J. Mod. Phys. A" **30**, 1543005 (2015).

[4] M. Neubert, "Adv. Ser. Dir. High Energy Phys." **15**, 239 (1998).

[5] N. Uraltsev, in *At the Frontier of Particle Physics*, edited by M. Shifman and B. Ioffe (World Scientific, Singapore, 2001), https://dx.doi.org/10.1142/9789812810458$_0$034.

[6] A. Lenz and T. Rauh, "Phys. Rev. D" **88**, 034004 (2013).

[7] M. Kirk, A. Lenz, and T. Rauh, "J. High Energy Phys." 12 (2017) 068; 06 (2020) 162(E).

[8] J. Gratrex, B. Melić, and I. Nišandžić, "J. High Energy Phys." 07 (2022) 058.

[9] Y. Aoki et al. (Flavour Lattice Averaging Group (FLAG)), "Eur. Phys. J. C" **82**, 869 (2022).

[10] R. Aaij et al. (LHCb Collaboration), "Phys. Rev. Lett." **119**, 101801 (2017).

[11] J. M. Link et al. (FOCUS Collaboration), "Phys. Rev. Lett." **95**, 052003 (2005).

[12] M. Iori et al. (SELEX Collaboration), “Phys. Lett. B” **523**, 22 (2001).

[13] M. Neubert, “Adv. Ser. Dir. High Energy Phys.” **15**, 239 (1998).

[14] H.-Y. Cheng, “J. High Energy Phys.” 11 (2018) 014.

[15] T. Abe (Belle II Collaboration), arXiv:1011.0352.

[16] K. Akai, K. Furukawa, and H. Koiso, “Nucl. Instrum. Methods Phys. Res., Sect. A” **907**, 188 (2018).

[17] A. Natochii, T. E. Browder, L. Cao, K. Kojima, D. Liventsev, F. Meier, K. R. Nakamura, H. Nakayama, C. Niebuhr, A. Novosel, G. Rizzo, S. Y. Ryu, L. Santelj, X. D. Shi, S. Stefkova, H. Tanigawa, N. Taniguchi, S. E. Vahsen, L. Vitale, and Z. Wang, “Beam background expectations for Belle II at SuperKEKB,” 2022. arXiv:2203.05731 [hep-ex].

[18] T. Keck, “FastBDT: A speed-optimized and cache-friendly implementation of stochastic gradient-boosted decision trees for multivariate classification,” arXiv:1609.06119 (2016).

[19] S. Longo et al., “CsI(Tl) pulse shape discrimination with the Belle II electromagnetic calorimeter as a novel method to improve particle identification at electron–positron colliders,” *Nuclear Instruments and Methods in Physics Research Section A: Accelerators, Spectrometers, Detectors and Associated Equipment* **982**, 164562 (2020).

[20] D. Brown, J. Ilic, and G. Mohanty, “Extracting longitudinal shower development information from crystal calorimetry plus tracking,” *Nuclear Instruments and Methods in Physics Research Section A: Accelerators, Spectrometers, Detectors and Associated Equipment* **592**, no. 3, 254–260 (2008).

[21] I. J. Good, "Rational Decisions," *Journal of the Royal Statistical Society. Series B (Methodological)* **14**, no. 1, 107–114 (1952), http://www.jstor.org/stable/2984087.

[22] T. Keck et al., "The Full Event Interpretation," *Computing and Software for Big Science* **3**, no. 6 (2019).

[23] G. C. Fox and S. Wolfram, "Observables for the Analysis of Event Shapes," *Phys. Rev. Lett.* **45**, 2480 (1980).